Tran-SET

Transportation Consortium of South-Central States

Solving Emerging Transportation Resiliency, Sustainability, and Economic Challenges through the Use of Innovative Materials and Construction Methods: From Research to Implementation

Field Retrofit and Testing of a Corroded Metal Culvert Using GFRP

Project No. 20STUNM30

Lead University: University of New Mexico

Final Report

March 2022

Disclaimer

The contents of this report reflect the views of the authors, who are responsible for the facts and the accuracy of the information presented herein. This document is disseminated in the interest of information exchange. The report is funded, partially or entirely, by a grant from the U.S. Department of Transportation's University Transportation Centers Program. However, the U.S. Government assumes no liability for the contents or use thereof.

Acknowledgements

The PIs would like sincerely to thank the contributions of our lab manager Mr. Kenny Martinez for his immense help with conducting the testing.

TECHNICAL DOCUMENTATION PAGE

1. Project No.	2. Government Accession No.	3. Recipient's Catalog No.
20STUNM30		

4. Title and Subtitle	5. Report Date
Field Retrofit and Testing of a Corroded Metal Culvert Using GFRP	03/21/2022
	6. Performing Organization Code
7. Author(s) PI: Mahmoud M. Reda Taha Co-PI: Susan Bogus Halter Mohammed Abdellatef Daniel Heras Murcia	**8. Performing Organization Report No.**
9. Performing Organization Name and Address Transportation Consortium of South-Central States (Tran-SET) University Transportation Center for Region 6 3319 Patrick F. Taylor Hall, Louisiana State University, Baton Rouge, LA 70803	**10. Work Unit No. (TRAIS)**
	11. Contract or Grant No. 669A3551747106
12. Sponsoring Agency Name and Address United States of America Department of Transportation Research and Innovative Technology Administration	**13. Type of Report and Period Covered** Final Research Report 08/10/2021
	14. Sponsoring Agency Code

15. Supplementary Notes

Report uploaded and accessible at Tran-SET's website (http://transet.lsu.edu/).

16. Abstract

One of the current pressing problem for all DOTs is the corrosion-oriented deterioration of the existing metal culverts. These metal culverts typically are designed for a life of 50 years. However, corrosion is making them last no longer than 30years. Here we propose use of Glass Fiber Reinforced Polymers (GFRP) pipe section as a fit-in GFRP profile liner for complete repair and rehabilitation of the corroded metal culvert with an expected life of 75 years. This is mainly because of the corrosion free nature of the GFRP material. In the current study, the design method for using glass fiber-reinforced polymer (GFRP) slip liner to retrofit CMP culvert is presented. Furthermore, this report presents field implementation of retrofitting of a 24 in corroded corrugated metal pipe embedded that is 25 ft span and buried below 18 of soil. The corroded corrugated metal pipe was retrofitted with a 22 in diameter GFRP slip liner. Load testing before and after the retrofitting proves the efficiency of the proposed retrofitting system and its ability to extend the service life of the retrofitted pipe.

17. Key Words	18. Distribution Statement
Culverts, Rehabilitation, GFRP, Composite action	No restrictions. This document is available through the National Technical Information Service, Springfield, VA 22161.

19. Security Classif. (of this report)	20. Security Classif. (of this page)	21. No. of Pages	22. Price
Unclassified	Unclassified	68	

Form DOT F 1700.7 (8-72) **Reproduction of completed page authorized.**

SI* (MODERN METRIC) CONVERSION FACTORS

APPROXIMATE CONVERSIONS TO SI UNITS

Symbol	When You Know	Multiply By	To Find	Symbol
		LENGTH		
in	inches	25.4	millimeters	mm
ft	feet	0.305	meters	m
yd	yards	0.914	meters	m
mi	miles	1.61	kilometers	km
		AREA		
in^2	square inches	645.2	square millimeters	mm^2
ft^2	square feet	0.093	square meters	m^2
yd^2	square yard	0.836	square meters	m^2
ac	acres	0.405	hectares	ha
mi^2	square miles	2.59	square kilometers	km^2
		VOLUME		
fl oz	fluid ounces	29.57	milliliters	mL
gal	gallons	3.785	liters	L
ft^3	cubic feet	0.028	cubic meters	m^3
yd^3	cubic yards	0.765	cubic meters	m^3
		NOTE: volumes greater than 1000 L shall be shown in m^3		
		MASS		
oz	ounces	28.35	grams	g
lb	pounds	0.454	kilograms	kg
T	short tons (2000 lb)	0.907	megagrams (or "metric ton")	Mg (or "t")
		TEMPERATURE (exact degrees)		
°F	Fahrenheit	5 (F-32)/9 or (F-32)/1.8	Celsius	°C
		ILLUMINATION		
fc	foot-candles	10.76	lux	lx
fl	foot-Lamberts	3.426	$candela/m^2$	cd/m^2
		FORCE and PRESSURE or STRESS		
lbf	poundforce	4.45	newtons	N
lbf/in^2	poundforce per square inch	6.89	kilopascals	kPa

APPROXIMATE CONVERSIONS FROM SI UNITS

Symbol	When You Know	Multiply By	To Find	Symbol
		LENGTH		
mm	millimeters	0.039	inches	in
m	meters	3.28	feet	ft
m	meters	1.09	yards	yd
km	kilometers	0.621	miles	mi
		AREA		
mm^2	square millimeters	0.0016	square inches	in^2
m	square meters	10.764	square feet	ft^2
m	square meters	1.195	square yards	yd^2
ha	hectares	2.47	acres	ac
km	square kilometers	0.386	square miles	mi^2
		VOLUME		
mL	milliliters	0.034	fluid ounces	fl oz
L	liters	0.264	gallons	gal
m	cubic meters	35.314	cubic feet	ft^3
m	cubic meters	1.307	cubic yards	yd^3
		MASS		
g	grams	0.035	ounces	oz
kg	kilograms	2.202	pounds	lb
Mg (or "t")	megagrams (or "metric ton")	1.103	short tons (2000 lb)	T
		TEMPERATURE (exact degrees)		
C	Celsius	1.8C+32	Fahrenheit	°F
		ILLUMINATION		
lx	lux	0.0929	foot-candles	fc
cd/m^2	$candela/m^2$	0.2919	foot-Lamberts	fl
		FORCE and PRESSURE or STRESS		
N	newtons	0.225	poundforce	lbf
kPa	kilopascals	0.145	poundforce per square inch	lbf/in^2

TABLE OF CONTENTS

LIST OF FIGURES

ACRONYMS, ABBREVIATIONS, AND SYMBOLS

W_c: Soil column load

H: Burial depth

γ_s: Unit weight of soil

d_0: the outside diameter of GFRP pipe

W_A: The soil arch load

VAF: Vertical Arching Factor

ϕ_s: Capacity modification factor for soil

M_s: Secant constrained soil modulus

R: Effective radius of pipe

A_i: Section area

E_g: Off-axis modulus of GFRP

S_h: Hoop stiffness factor

T_1: Pipe wall factor thrust

P_i: Live load transferred from HS-25

C_i: Live load distribution coefficient

P_W: Hydrostatic pressure at the spring line

A_r: Pipe wall area

ϕ_p: Capacity modification factor for pipe

F_g: Tensile strength of GFRP

T_{cr}: Critical wall thrust

f_{cr}: Critical buckling resistance

M_s: Secant constrained soil modulus

B: Nonuniform stress distribution factor

I_g: Moment of inertia

R_w: Water buoyancy factor

Δ_y: Pipe deflection

D_1: Deflection lag factor

K_c: Bedding factor

PS_g: Pipe stiffness of GFRP

W_1: Live load

E_S: Modulus of soil reaction

Δ: pipe deflection due to bending

Δ_c: Construction induced pipe deflection

D_m: Mean pipe diameter

γ_p: Load factor for vertical earth pressure

ε_{bu}: Factored bending strain

D_f: Shape factor

γ_b: Load factor for combined strain

C_g: Distance from the inside diameter to the neutral axis

Q_s: Hydraulic capacity of the pipe

n_s: Manning's roughness coefficient

R_s: Hydraulic radius

S: Pipe slope

EXECUTIVE SUMMARY

Metal culverts have served as a common structural element in highway design since the mid-1950s because of their low initial cost, ease of fabrication, and simple construction method. There has been an epidemic of corrosion of metal culverts for the last decade. Such corrosion results in loss of cross- section and occasionally leads to structural failure of the culvert. Numerous failures have taken place imposing a high cost with the need to rebuild many culverts in addition to significant indirect costs associated with highway closure. Glass fiber reinforced polymers (GFRP) have become a desirable material for structural strengthening and rehabilitation over the past two decades. Prior research supported by TranSET showed that GFRP profile liner can retrofit an existing metal culvert and provide structural capacity for the corroded metal culvert to extend its service for 50-100 years. New Mexico Department of Transportation (NMDOT) allocated a field trial site for experimentation of the technology. A mock road resembling a two-lane rural road with an 18-inch backfill above a 25-foot long and 24-inch diameter corroded metal culvert has been prepared by NMDOT. Field implementation was executed using 22 in GFRP pipe slip lined and grouted to the existing corroded corrugated metal culvert. Load testing was performed to ensure the integrity of the retrofitted culvert. This report describes the design process, the field experimentation steps, and the retrofitting process. The report also describes the load testing and the monitoring of the retrofitted metal pipe using the fit-in GFRP profile liner technology.

IMPLEMENTATION STATEMENT

New Mexico Department of Transportation (NMDOT) allocated a corroded corrugated metal culvert in La Mesita Patrol yard in NMDOT Area 6. The corroded corrugated metal culvert was made available for field implementation of the GFRP technology. The PI designed and implemented the fit-GFRP profile liner to retrofit the corroded metal pipe. Instrumented field testing of the retrofitted culvert was performed to ensure proper repair and to observe the post-repair behavior. The PI firmly believes that the outlined strengthening scheme can be effectively implemented in the field for extending the service life of existing metal culverts 75 years post repair.

1. INTRODUCTION

1.1RESEARCH NEED AND SIGNIFICANCE

Metal culverts are flexible long-spanning piped structures that facilitate the smooth conveyance of water without disturbing the flow or impacting the ecosystem. Typically, these structures are used for storm sewers, underpasses, railway, and highway bridges. Metal culverts are usually prefabricated using curved metal plates and connected using a locked seam [1]. Subsequently, the piped structures are buried with a backfill for easy transfer of the loads and for providing stability to the culvert structure itself. Metal culverts are mostly made of steel and aluminum. Because of ease of installation and low cost of fabrication, metal culverts have gained wide acceptance since the mid-1950s. Metal culverts have also been fabricated in different desired shapes with constant radius circles, ellipse in horizontal or vertical directions, and arched pipe, as shown in Figure 1 [*2*].

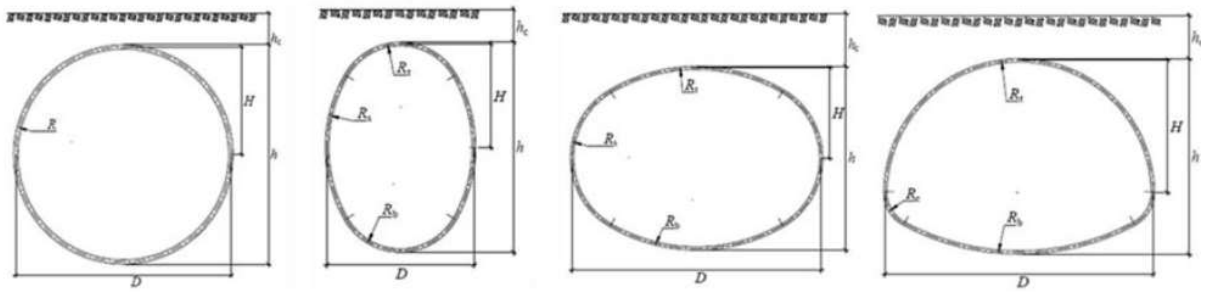

FIGURE 1 Different profiles for metal culverts buried in soil [2]

According to the U.S. Federal Highway Administration (FHWA), a total number of 118,394 culverts are part of the U.S. bridge inventory [3]. These culverts are constructed either using concrete or corrugated steel. However, literature reports that the actual numbers are much higher, and several departments of transportation (DOTs) are in the process of inventory investigations to assess the real number of existing culverts [4]. It was also reported that there were several defects of corroded metal pipe (CMP) observed in the field, such as shape distortion, misalignment, joint defects, seam defects, circumferential seams, localized damage and dents, and durability problems [5]. Many of these defects can be tied to the corrosion problem of CMP. Corrosion of metal culverts has been a considerable challenge as it excessively lowers their life expectancy and significantly affects their serviceability [6]. Most of the culvert failures can be attributed to corrosion. This is normally caused by the contaminants in the backfill soil and the aggressive nature of flowing water along with the soil cover around the culverts [7,8]. Literature shows that life expectancy for metal culverts is around 50 years [9]. However, heavy corrosion dropped this life expectancy to lower than 30 years, creating significant financial overburden on metal culverts [9]. A Transportation Research Board (TRB) report in 2004 indicated that the failure of metal culverts had been significantly increasing all over the country, which is a relatively expensive event. The high cost attributed to rebuilding failing metal culverts is not only related to material and construction costs but also associated with road closures and traffic delays [10]. Therefore, retrofitting metal culverts is a viable alternative when compared with metal culvert replacement.

1.2 REPORT ORGANIZATION

This report is subdivided into five chapters. Chapter 1 presents an introduction and objectives. Field implementation of GFRP retrofit technique is presented in Chapter 2. Chapter 3 includes the findings made during field implementation. Chapter 4 describes the design methodology and guidelines for structural design and field implementation. Chapter 5 summarize the conclusions of the report.

2. OBJECTIVES

The objective of this research project is to conduct full-scale field implementation and testing of the field retrofit of CMP using GFRP slip-lining and provide an implementation guidebook for future application. This report provides information on the technical aspects of the above project including:

- Structural design of GFRP liner retrofit for a field corroded metal culvert.
- Field application of GFRP profile liner to retrofit corroded metal culvert.
- Monitoring the behavior of the retrofitted CMP-GFRP culvert subjected to traffic loads.

3. LITERATURE REVIEW

The four most common techniques for retrofitting metal culverts are slip-lining, cured in place, sprayed-on liners, and pipe bursting. Among the presented techniques, as shown in Figure 3, slip-lining is the most commonly used technique for the comprehensive retrofit of metal culverts. The challenge is that when a metal liner is used, it is still prone to corrosion as depicted in Figure 2. Materials like PVC pipes and high density polyethelene (HDPE) pipes have gained acceptance as slip-lining materials [11]. The literature identifies that HDPE, being a thermoplastic, viscoelastic material, has a significantly low long-term strength [4]. Moreover, several reports indicated problems with HDPE and PVC pipes when used for new culverts [12,13]. A study investigated 191 HDPE pipelines in 10 U.S. states and found that the structural health of all the tested culverts was well below acceptable service levels [12].

(a) (b)

FIGURE 2 Failure of corroded metal culverts [2].

FIGURE 3 Culvert retrofit using HDPE pipes [2].

It is also important to consider the hydraulic capacity of culverts before conducting a retrofit for an existing culvert. The pipes currently used for retrofitting, such as HDPE and glass fiber reinforced polymer (GFRP) filament wound sections, have a much lower surface roughness

coefficient. Surface roughness is typically identified in the form of a Manning's coefficient. Manning's coefficient of a CMP is 0.022, which is typically the host pipe, and Manning's coefficient for GFRP is as low as 0.009, and for other thermoplastic pipes is in the same order. The literature indicates no loss or increased hydraulic capacities can be achieved by using GFRP [8]. Several field investigations were conducted to study Manning's coefficients, and the effect of thermoplastic smooth slip-lining materials for retrofit corrugated metal pipes was higher or equivalent to the cost of higher diameter pipes [8,14].

With improved manufacturing techniques and lower costs, GFRP has emerged as a desirable material for structural applications. GFRP is essentially corrosion-free as it has no electrochemical effect. This makes GFRP a preferred material over steel for structures serving in harsh environmental conditions. Fiber reinforced polymer (FRP) has gained wide acceptance for retrofitting existing structures (bridges and buildings) because of ease in installation and the high strength-to-weight ratio [15]. Shear and flexural strengthening for structural concrete using FRP has become standard practice in today's market. Design guidelines using FRP in concrete structures are detailed by the American Concrete Institute [16]. However, using FRP to retrofit metal culverts is relatively new, and very few investigations have been completed. This report discusses the use of GFRP as a potential material for retrofit of corroded CMP culverts. The method of designing GFRP slip liner pipe for retrofitting a 25 ft corroded metal CMP culvert is discussed. A finite element (FE) model is developed to investigate the retrofitted culvert response under service conditions including standard traffic loads.

After designing the GFRP pipe required to retrofit the corroded culvert, the FE model was used to investigate the level of strains expected during testing. The corroded culvert was then tested via a truckload after burial, then the GFRP pipe was slip-lined and finally tested again with the truckload to ensure structural integrity.

4. METHODOLOGY

4.1STRUCTURAL DESIGN OF GFRP LINER RETROFIT FOR A FIELD CORRODED METAL CULVERT

The GFRP slip liner's design follows AASHTO Load and Resistance Factor Design (LRFD) for new culverts [19], discarding any structural contribution from the existing corroded culvert. The soil loads are calculated using soil column load and soil arch load techniques. The soil column load is the weight of the soil directly above the pipe, calculated as $W_c = \gamma_s . H . d_0$, where, H is burial depth (ft.), γ_s is the unit weight of soil (pcf), and d_0 (in) is the outside diameter of GFRP pipe. The soil arch load W_A (psi) is calculated using the Vertical Arching Factor (VAF). This factor reduces the load proportional to the stiffness of the pipe. The soil arch load could be calculated as:

$$W_A = P_{sp} . VAF \tag{1}$$

$$P_{sp} = (\gamma_s) . (H + 0.11 d_0) \tag{2}$$

$$VAF = 0.76 - 0.71 \left(\frac{S_h - 1.17}{S_h + 2.92}\right) \tag{3}$$

where: ϕ_s = Capacity modification factor for soil, M_s = Secant constrained soil modulus (psi), R = Effective radius of pipe (in.), A_i = Section area ($in.^2$), E_g = Off-axis modulus of GFRP (psi), and S_h = Hoop stiffness factor. The design traffic is conducted using the AASHTO HS-25 wheel load configuration [19]. The current structural design is based on the direct burial approach based on AASHTO LRFD section 12 design criteria [19]. The current design is developed based on four critical failure mechanisms, illustrated in Figure 4: wall thrust, wall buckling, deflection, and bending strain. Besides the structural design, the hydraulic design should be satisfied as well. The values used for this report and given GFRP pipe (thickness of 0.35 in) are an off-axis modulus of 1088 ksi and tensile strength of 5500 psi.

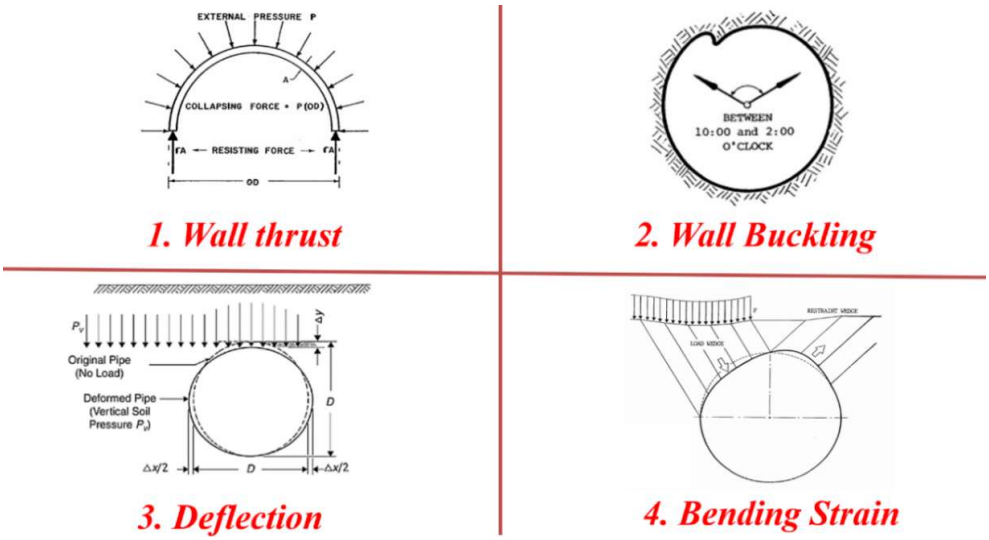

FIGURE 4 Structural design criteria for culvert pipes

4.1.1 Wall Thrust

The stress in the pipe wall is determined based on the total live load and the dead load acting on the pipe. The pipe wall factor thrust demand could be calculated as:

$$T_1 = 1.3(1.5W_A + 1.67.P_i.C_i + P_w).\left[\frac{d_0}{2}\right] \quad (4)$$

where, P_i is the live load transferred from HS-25 (lbf), C_i is the live load distribution coefficient, and P_W is the hydrostatic pressure at the spring line (psi). Based on pipe wall factored resistance, the wall area can be decided for the pipe wall. The required GFRP thickness can be calculated as:

$$t_{GFRP} = \frac{T_1}{\phi_p.f_g} \quad (5)$$

where, T_1 is the calculated wall thrust, ϕ_p is the capacity modification factor for pipe, F_g is the tensile strength of GFRP (psi). The GFRP pipe thickness shall be rounded to one quarter of an inch. The values used for this report and given GFRP pipe (thickness of 0.35 in) are with an off-axis modulus of 1088 ksi and tensile strength of 5500 psi.

4.1.2 Wall Buckling

The buckling of the pipe wall is a function of the pipe's wall properties and the off-axis modulus of elasticity of the pipe material. To demonstrate buckling resistance, the pipe wall capacity must be greater than the tensile strength of the pipe. If the critical buckling stress is lower than the tensile strength of GFRP, then wall thrust shall be recalculated based on buckling resistance. The critical buckling resistance for a unit length of the pipe can be calculated as:

$$f_{cr} = 9.24.\frac{R}{A_i}.\left[\sqrt{B.R_w.\phi_s.M_s.\left[\frac{E_g.I_g}{R^3}\right]}\right] \quad (6)$$

where, M_s is the secant constrained soil modulus (psi), R is the effective radius of pipe (in), B is the nonuniform stress distribution factor, I_g is the moment of inertia ($\frac{in.^4}{in.}$), E_g is the off-axis modulus (psi), R_w is the water buoyancy factor, and ϕ_s is the resistance factor for soil stiffness.

4.1.3 Deflection

The change in diameter of the pipe under the soil and live loads is considered as pipe deflection. The vertical dimension of the pipe is limited to a deflection of 7.5% of the base inside diameter. The pipe deflection is a function of the pipe stiffness. The pipe stiffness for the GFRP pipe could be estimated as in [17]. The pipe deflection of a unit length of the pipe can be calculated as:

$$\Delta_y = \frac{K_c[(D_1)(W_c)+W_1]}{(0.419)(PS_g)+(0.061)(E_S)} \quad (7)$$

where, D_1 is the deflection lag factor, K_c is the bedding factor, PS_g is the pipe stiffness of GFRP (psi), W_1 is the live load (lbf/in), and E_S is the modulus of soil reaction (psi).

If corrosion and loss of a section of the existing culverts took place, the soil above the culvert might have moved and caused voids/gaps above the culvert, the Engineer shall consider designing the GFRP section to accommodate the unbalanced loading associated with voids in the soil.

4.1.4 Bending Strains

AASHTO design method requires that the bending strain shall be evaluated and within the permissible strain limits of the GFRP pipe section. The deflection of a unit length of the due to bending (Δ) can be evaluated as:

$$\Delta = \Delta_c . D_m - \left(\frac{T_1 D_m}{A_i E_g \ _p}\right) \tag{8}$$

Where, Δ_c is the deflection of pipe (in), construction induced deflection, limit 5%, D_m is the mean pipe diameter (in.), γ_p is the load factor for vertical earth pressure, E_g is the off-axis modulus (psi). The factored bending strain could be calculated as:

$$\varepsilon_{bu} = \gamma_b . D_f \left(\frac{C_g}{R}\right)\left(\frac{\Delta}{D_m}\right) \tag{9}$$

where, D_f is the shape factor, γ_b is the load factor for combined strain, R is the effective radius of pipe (in), D_m is the mean pipe diameter (in), and C_g is the distance from the inside diameter to the neutral axis (in). The off-axis modulus shall be provided by the manufacturer. Standard GFRP pipe design values for thicknesses up to 1.00 in are with an off-axis modulus of 1088 ksi and tensile strength of 5500 psi. Alternatively, the designer might obtain specific values for the off-axis modulus and the tensile strength from the GFRP manufacturer.

4.1.5 Hydraulic Design

It is crucial to consider the hydraulic capacity of culverts before conducting a retrofit for the existing culvert. The reduction in hydraulic radius is a common phenomenon of slip lining a culvert. However, the pipes currently used for retrofitting, such as HDPE and GFRP filament wound sections, have a much lower surface roughness coefficient. This is typically identified in the form of a Manning's coefficient. The hydraulic capacity of the pipe is calculated based on Manning's equation for gravity pipe flow as:

$$Q_s = \left[\frac{1.49}{n_s} . A_s . R_s^{\frac{2}{3}} \sqrt{S}\right] \tag{11}$$

where, Q_s is the hydraulic flow in (cfs), n_s is Manning's roughness coefficient, R_s is the hydraulic radius and S is the slope. Manning's coefficient for the corrugated metal pipe is 0.024, and for the GFRP pipe is 0.00914.

GFRP has shown an excellent abrasion behavior and wear resistance [20]. GFRP used for water tanks with stringent leakage performance demands have shown a minimum life expectancy of 30 years. Expected service life of the GFRP retrofit is 50-75 years.

4.2 FIELD APPLICATION OF GFRP PROFILE LINER TO RETROFIT CORRODED METAL CULVERT

The design method was applied for future implementation on a steel CMP of 25 ft, shown in Figure 5. The steel pipe had a nominal diameter of 24 in, and an average corroded thickness of 0.05 in. The retrofitted pipe will be buried under 18 in of soil, with a slope of 0.001. A grout thickness of 1.5 inches was assumed, resulting in a GFRP outside diameter of 21 in. The culvert was provided by NMDOT in La Mesita Patrol Yard.

FIGURE 5 Corroded metal steel pipe

The design process is iterative in nature to find the optimal GFRP thickness to satisfy all design requirements. For a GFRP thickness of 0.35 in, with an off-axis modulus of 1088 ksi and tensile strength of 5500 psi:

1) Pipe thrust was found to be $T_1 = 535.7$ lb/in, with a factor of safety of 3.6 against chosen thickness,

2) The critical buckling resistance was found to be $f_{cr} = 6.1$ ksi, with a factor of safety of 1.1 against tensile strength,

3) The deflection $\Delta_y = 0.7$in, with a factor of safety of 2.3 against the deflection limit,

4) The maximum bending strain 0.5%, with a factor of safety of 1.2 against the ultimate GFRP strain, and

5) Hydraulic capacity of 6.53 cfs, which is larger than the original hydraulic capacity of CMP pipe of 3.89 cfs.

4.3 NUMERICAL MODELING

Two FE models of the CMP and CMP-GFRP composite section were developed using ABAQUS simulation environment. Both models aim to estimate the strains in the CMP and CMP-GFRP under service loading conditions. The models were developed making use of the 3D geometry in ABAQUS. Since CMP would be buried in a semi-infinite soil space, and the load redistribution is expected to take place over cover depth, the models were constructed with a soil volume extending 8 times the soil cover in all directions of the pipe, as shown in Figure 6. The soil modulus was assumed to be 13 ksi. The element used to represent the soil was a 3D solid element. The CMP was modeled using a shell element with a thickness of 0.05. Since the pipe is corrugated, a reduced elastic modulus of 8000 ksi was assumed to account for additional deformation [2,17]. Poisson's ratio was assumed to be 0.26. The CMP elements were constrained via an embedment constraint to the soil elements adjacent to them. The grout was modeled using 3D solid elements, with a thickness of 1.5 in, and isotropic material with a modulus of elasticity of 3625 ksi. The GFRP pipe is also modeled as a 3D solid element with a thickness of 0.35 in. The material used for GFRP was modeled using a composite layup toolbox in ABAQUS. The composite layup was been carried out in 10 layers with a repeated inner layup of +45° and -45°, in between outer layers of 0°.

The material properties for the GFRP pipe section were defined based on the orthotropic elastic properties based [2]. Service loads were applied as two wheels, 16 kips each representing HS-20 truck. Each wheel was presented by a ramping pressure of 80 psi over an area of 20 in x 10 in, placed 3 ft from the center of the pipe, as shown in Figure 6. It was expected that at this service load, all materials will exhibit elastic response [18]. Finally, tie constraints were implemented between GFRP-grout-CMP, assuming a perfect bond between them. Since the model was only subjected to service loading conditions, elasticity was assumed for all materials involved.

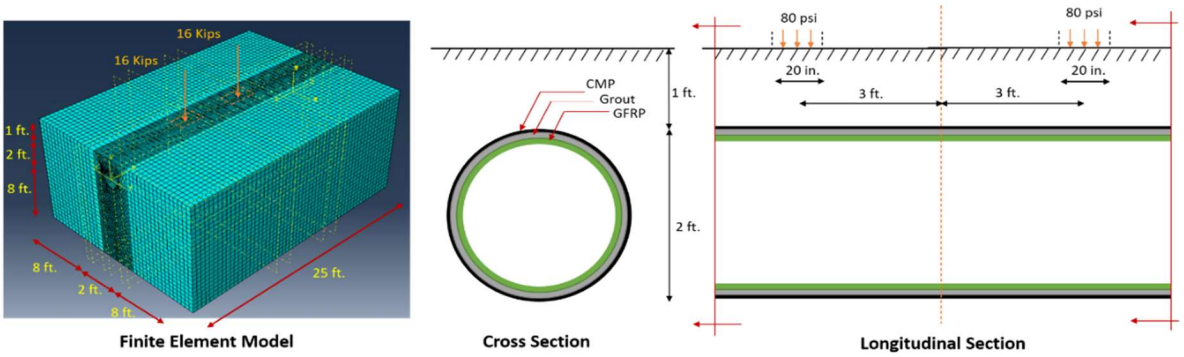

(a) (b) (c)

FIGURE 6 Finite element model of the GFRP slip-liner (a) and illustrative sections (b and c).

Figure 7 shows the strain results of the CMP model. As expected from the literature, the dominate response could be observed in a high level of tangential strains under wheel positions. It is also important to note that, because of the flexibility of the culvert, longitudinal strains were also present, reflecting a flexural-like response for the culvert. Figure 8 shows the strain results in the GFRP pipe of the CMP-GFRP model. It can be observed that the magnitude of strains in this model is lower than the previous model, due to the reinforcement and composite action via adding the GFRP pipe. Similar to the previous model, the tangential strains were higher than longitudinal strains.

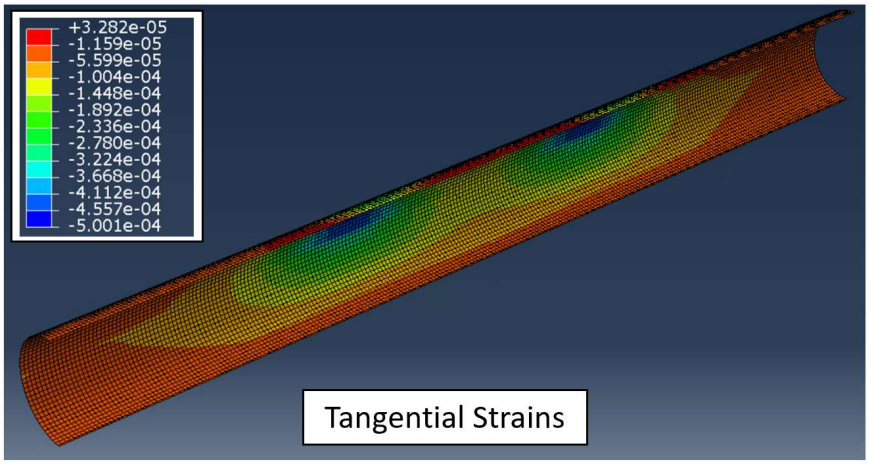

(a)

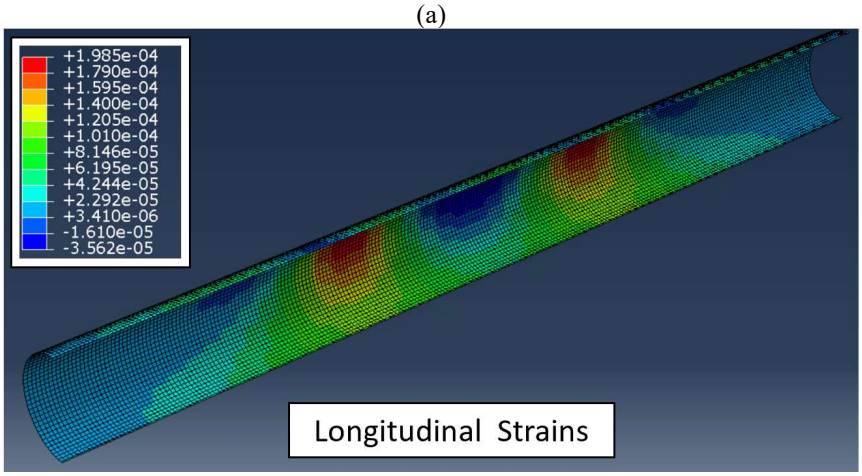

(b)

FIGURE 7 Steel strain for CMP model. (a) tangential strains. (b) longitudinal strains.

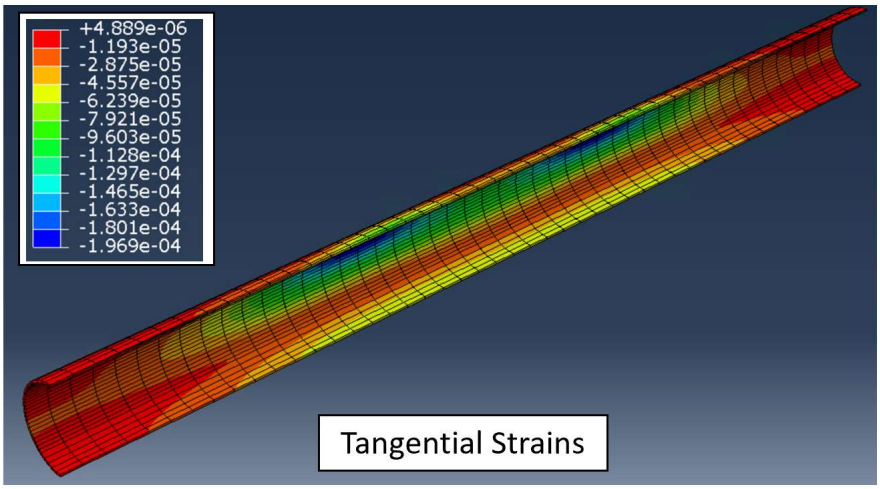

(a)

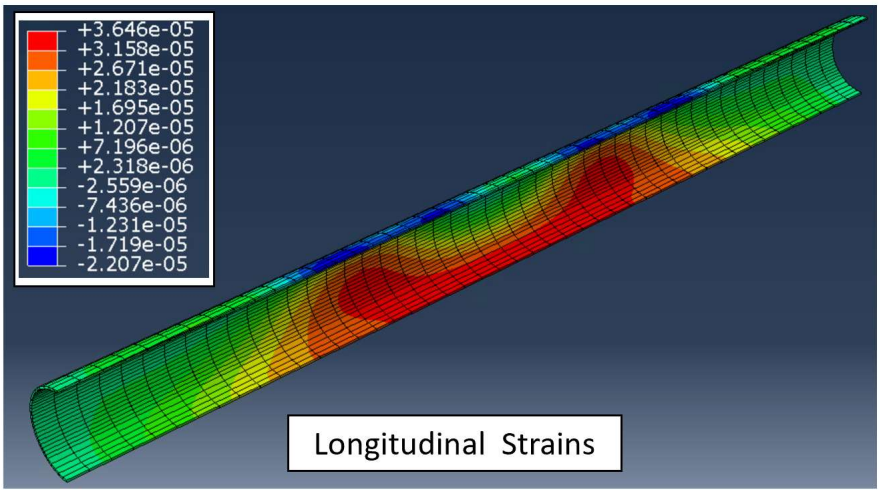

(b)

FIGURE 8 GFRP strains for CMP-GFRP model. (a) tangential strains. (b) longitudinal strains.

4.4 FIELD IMPLEMENTATION GUIDELINES OF GFRP LINER RETROFIT FOR A FIELD CORRODED METAL CULVERT

Once the structural design has been performed, a new pipe that is smaller in diameter than the host pipe is slid inside the existing host pipe. The annular space between the host pipe and the slip liner will then be filled using a polymer-based grout material. Once the grout material is cured, the culvert is ready for service. Essentially any pipe material can be used as the slip liner. This document is focused on using GFRP pipes. CMPs are the prominent materials used for the slip-lining technique. Below are the outlined steps for the slip-lining process:

- Inspect the culvert for any diameter changes along the length of the culvert, connections, protrusions, and sediments. This step is critical to ensure that the slip lining GFRP pipe will fit inside the host pipe. The presence of sediments can potentially affect the bond between the host pipe and the GFRP slip lining pipe.
- Prior to starting the work, the engineer and the contractor shall review the 2014 Edition of the New Mexico Department of Transportation Standard Specifications for Highway and Bridge Construction and the 2017 Special Provision for Section 570-B: Culvert Slip Lining.
- Determine the diameter of the GFRP slip line pipe. Based on the field implementation, it is recommended to use a 2-inch minimum annular space. This means a 4-inch total difference in diameter between the GFRP pipe and the existing culvert shall be used. This spacing should account for protrusions in the hosting pipe.
- If corrosion and loss of a section of the existing culverts took place, the soil above the culvert might have moved and caused voids/gaps above the culvert. the Engineer shall consider designing the GFRP section to accommodate the unbalanced loading associated with voids in the soil.
- For long culverts (longer than 10 ft.), the GFRP slip lining pipe shall be divided into segments. Each of these segments shall not exceed 10 ft. The segments must be connected with polymer-based material as specified by the manufacturer. This step might be done prior to the slip lining process. For very long stretches, the segments could be joined as slip lining proceeds. The contractor needs to inspect the connected GFRP pipe to ensure proper sealing takes place.
- Approval of the GFRP materials by EPA might be necessary if running water is to pass through this GFRP retrofit.
- Clean the host culvert to clear out any sediments present.
- Control the water passage by setting up a flow bypass where necessary.
- Any necessary repairs for the existing culvert must be conducted prior to slip lining. Such repairs include embankment repairs, identifying and filling the voids.
- Construct a guide path to ensure the location and facilitate the slip-lining of the GFRP pipe into the host pipe.
- Based on the total length of the GFRP pipe, it might be necessary to use a forklift to transport and align the GFRP pipe at the entrance of the culvert.
- A thin wood plate might be needed to exert uniform pressure at the GFRP pipe end to allow its slip lining into the culvert. Hydraulic equipment might also be used to exert this pressure. The above condition will only be needed if a tight annular space is developed. Providing a 2-inch annular spacing between the GFRP pipe and the existing culvert, as pointed out above, shall avoid the need for exerting pressure to slip line the GFRP pipe.

- Spacers at the top might be needed to prevent the GFRP pipe from moving upward due to the buoyancy of fresh concrete. The contractor will need to address the issue of buoyancy, and to making sure, the GFRP pipe is aligned.
- Install the continuous slip liner into the host pipe. Rigorous alignment of the GFRP slip lining pipe must be performed prior to the placement inside the host culvert. It is possible to connect the joints while sliding the GFRP inside the existing culvert. The contractor needs to inspect the connected GFRP pipe to ensure proper sealing takes place.
- A 24-hour relaxation period is recommended upon completion of slip-lining, followed by inspection for any leakages or other tests where necessary.
- Stabilize end injection and purging pipes for the grout and fill the annular space with a polymer grout material and allow it to cure.
- The polymer grout shall incorporate aggregate to reduce shrinkage. Sand with a nominal maximum size of 5 mm (# 4) must be used as a filler.
- If a relatively thin annular space (less than 1/2 inch) is to be filled, a polymer grout without a filler might be used.
- Restore the flow and perform site cleanup as necessary.

5. ANALYSIS AND FINDINGS

5.1 FIELD APPLICATION OF GFRP PROFILE LINER TO RETROFIT CORRODED METAL CULVERT

Coordination with NMDOT department personal followed the proposed plan. The final project plan is shown in Figure 9. First, the corroded metal pipe was instrumented on May 20th, 2021. Following that, the corroded metal pipe was buried prior to load testing. The testing was performed on May 28th, 2021. The GFRP pipe was moved to the site, instrumented, and connected on July 7th, 2021. The GFRP piper was slipped in the corroded metal culvert on July 13th, 2021. The polymer was pumped in between the two pipes to ensure structure integrity on July 14th, 2021. Finally, the retrofitted pipe was tested on July 21st, 2021. In the following sections, each of the tasks are explained in detail.

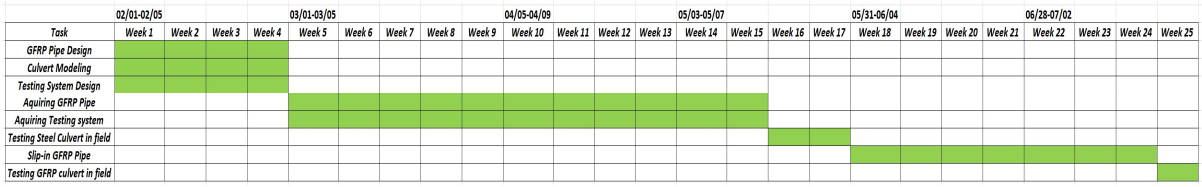

FIGURE 9 Final Testing Plan

5.2 INSTALL GFRP PIPE AND INSTRUMENTATION SENSORS

5.2.1 Corroded Metal Culvert Instrumentation

The corroded metal culvert was planned to be instrumented via strain rosettes, to measure both longitudinal and tangential strains, at three different locations. The locations of interest are at the center of the pipe and 6 ft from each side, aligning with the positions of the truck wheels, during load testing. At each of the locations, as shown in Figure 10, 3 strain rosettes are placed at the section top, bottom, and side, to evaluate the strain profile during loading.

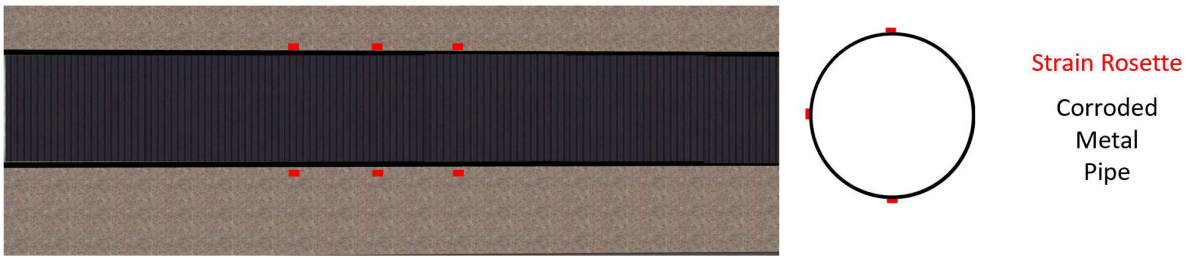

(a) (b)

FIGURE 10 Schematic of the corroded metal pipe instrumentation. (a) longitudinal view. (b) transversal view

Upon arrival to the NMDOT La Masita Yard, the corroded metal culvert was moved to a a shed to install the strain gauge sensors, as shown in Figures 11 and 12. The culvert pipe was cleaned from dust and rust and was ground at the planned sensor locations. The sensors were soldered on the cleaned surface. After all sensors were placed, the pipe was buried under 18 in of soil before load testing.

FIGURE 11 Corroded metal pipe before and after instrumentation

FIGURE 12 Instrumentation of corroded metal pipe

5.2.3 Corroded Metal Culvert Load Testing

After the corroded corrugated metal pipe was buried at a depth of 18 inches, as shown in Figure 13, load testing was performed. Before testing, the truck was weighed on a weighing scale, as shown in Figures 14 and 15. First, an empty truck with a total weight of 25.75 kips traveled over the center of the culvert, with the wheels aligned with the exterior sensor arrays. The truck was then filled with sand, to a total weight of 48.55 kips, and traveled on the same path over the culvert. Finally, the loaded truck traveled near one of the ends of the culvert, with the interior wheels of the truck aligned with the exterior array of sensors. The breakdown of each wheel load is presented in Figure 16.

FIGURE 13 Buried corroded metal pipe

(a) (b)

FIGURE 14 Weighing scale used to weight the test truck before and after filling it with sand. (a) scale installation. (b) scale after being wired.

(a) (b) (c)

FIGURE 15 Corroded corrugated metal culvert buried (a), load testing (b) truck getting filled with sand, (c) truck passing over culvert.

Figure 17 shows a sample of longitudinal and tangential strains for each load case. The arrival of the first and second axels of the truck could be observed in the spike and dilation of the measured strains. The results show the sustainability of the CMP to vibrations due to truck loading, as present in the signal noise. Also, the loaded truck case has higher strains than the unloaded case, specifically near the top of the corroded metal culvert. Finally, the loaded culvert observed significant strains in both longitudinal and tangential directions, not only in the tangential direction. This might be attributed to the fact that the culvert was buried at a relatively close distance of 18 inches from the surface. The full data from this testing is presented in Appendix A, Figures A-1 to A-24. The strains measured were consistent with the range of strains predicted by the FE model, which were in the order of 50-100 microstrains.

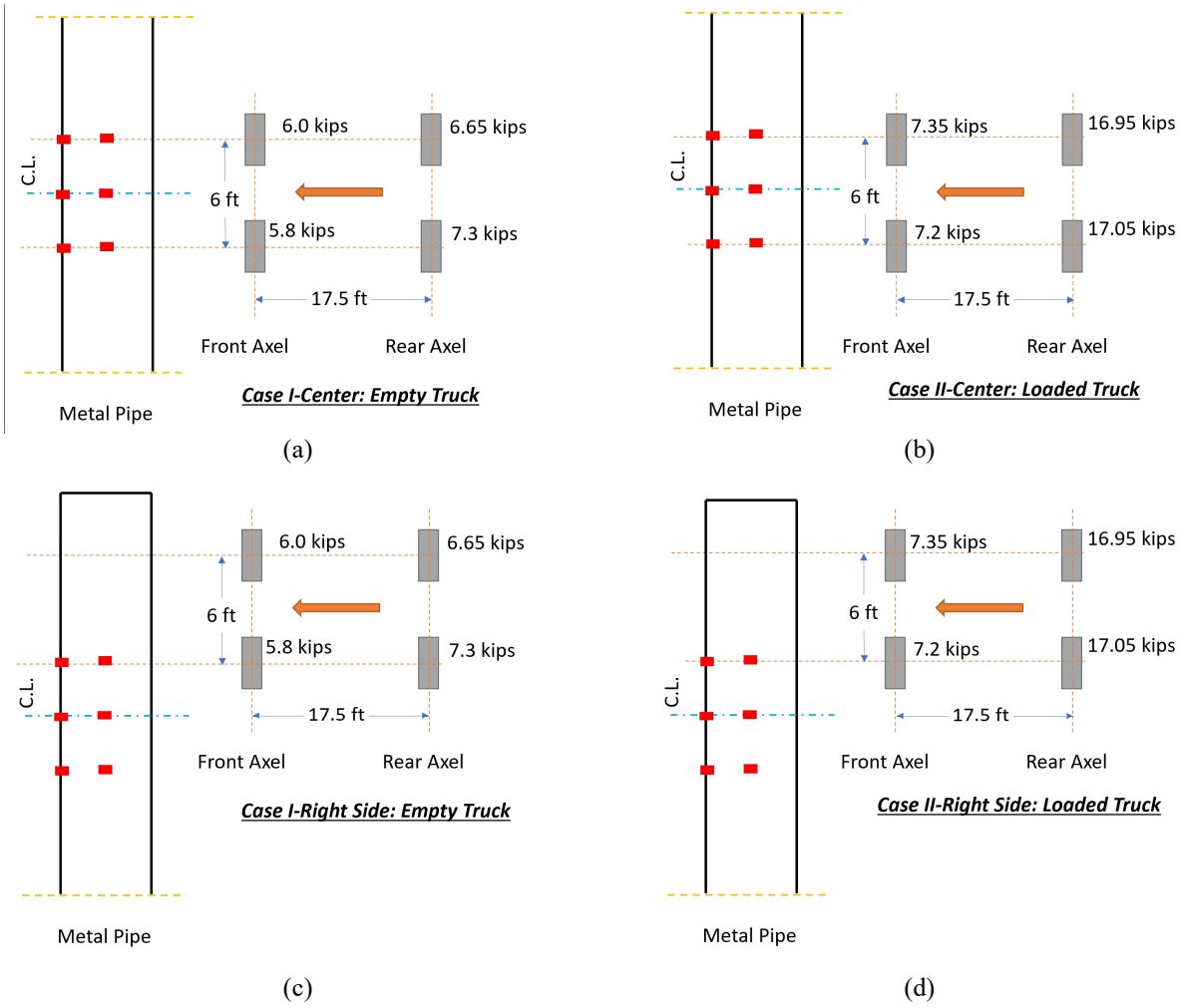

FIGURE 16 Load testing cases for corroded corrugated metal culvert buried at 18 inch depth. (a) Case I-center. Empty truck. (b) Case II-center. Loaded truck. (c) Case I-right side. Empty truck. (d) Case II-right side. Loaded truck.

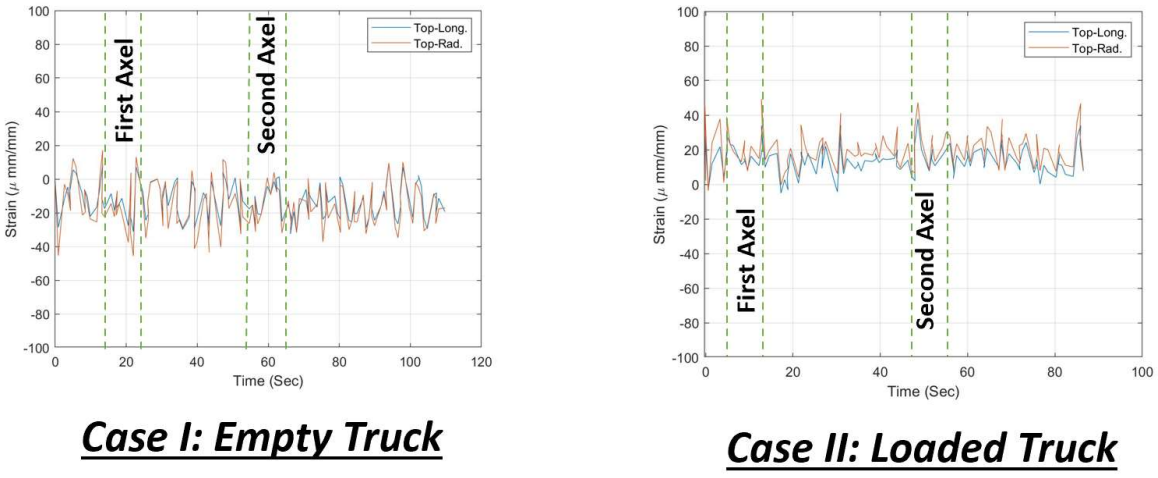

(a) (b)

FIGURE 17 Corroded metal culvert loading test sample data. Strains represented in microstrains (1 me = 10-6 e). (a) Case I. Empty truck. (b) Case II. Loaded truck.

5.2.4 GFRP Pipe Instrumentation

The manufactured GFRP pipe had an outer diameter of 20.125 in, and thickness of 0.5625 in, a little exceeding the required design criteria. The main reason for accepting this pipe was the reduced cost of manufacturing a pipe with this diameter since a smaller diameter pipe would have required a special mold. The GFRP pipe was delivered to the UNM team in 3 segments, each was 8 ft long, as shown in Figure 17. The middle segment was instrumented in the UNM structural laboratory, prior to moving to the NMDOT yard. Strain gauges were installed in the same locations indicated above for strain gauges installed on the corroded metal pipe.

Upon arrival at the NMDOT yard, the GFRP pipe pieces were moved to a shed to install the joints using polymer composite compatible with the GFRP material. The pipe was left for 24 hours to cure. As shown in Figure 18, after the joints cured and hardened, the wires of all sensors were secured and extended to the ends of the GFRP pipe, before the GFRP pipe was transported with a forklift to be installed for the slip-lining process.

(a)

(b)

(c)

FIGURE 18 GFRP pipe (a)-(b): Transportation of 3 GFRP sections to NMDOT yard (c) instrumentation and connecting the GFRP pipe segments.

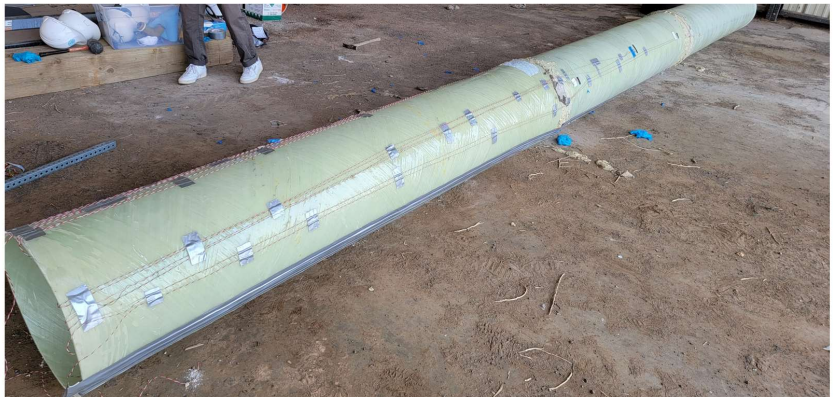

(a)

(b)

FIGURE 19 (a) Final instrumented and connected GFRP Pipe Before Slip-Lining. (b) Transporting integrated GFRP pipe to slip-lining location.

5.2.5 GFRP Pipe Slip-Lining

The instrumented and integrated GFRP pipe was transported using a forklift to the location of slip-lining, as shown in Figure 19. It was then carefully aligned and placed in an extended trench created ahead at the culvert front, such that it could be aligned with the buried corrugated metal pipe.

(a)

(b)

FIGURE 20 (a) Transporting GFRP pipe to slip-lining location (b) aligning and placing the GFRP pipe at slip-lining location.

Due to the small tolerance of the GFRP diameter and the corrugated metal culvert diameter, the GFRP pipe was driven by an excavator's small bucket to slide inside the metal pipe. After the GFRP pipe was placed fully inside the corroded corrugated metal pipe, the ends were sealed with an expansive foaming agent, in preparation for grout pumping then load testing, Figure 20. After placement of the GFRP pipe, the sensor alignment was as shown in Figure 21.

(a) (b) (c)

(d) (e)

FIGURE 21 (a)-(c) Slip-Lining Process driving the GFRP pipe inside the corrugated metal culvert. (d)-(e) GFRP pipe completely slid inside the corrugated metal culvert and application of the closure foam prior to grouting of the annular space.

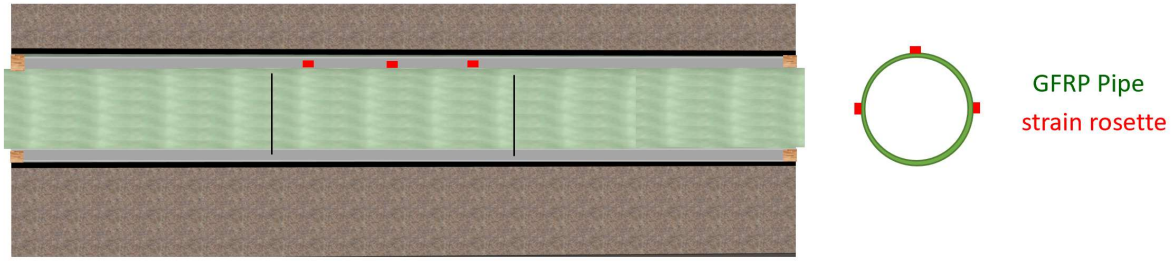

(a) (b)

FIGURE 22 Schematic of the GFRP pipe instrumentation. Longitudinal (a) and transversal (b) view.

Typically, fine aggregate is mixed with the polymer to reduce shrinkage of the grout. Due to the relatively small annular space, it was decided to grout the annular space between the GFRP pipe and the corrugated metal pipe using the polymer only. The polyester-based polymer was mixed and injected using a grout pump, as shown in Figure 22. Pumping was initiated at an opening created at the top of the metal pipe at mid span and continued until the polymer overflowed from both ends of the culvert. Overflow was allowed to take place for a few minutes to ensure all the annular space was filled with the polymer. Thin rods were inserted in the annular space at different heights and ensured all the annular space was filled with the polymer.

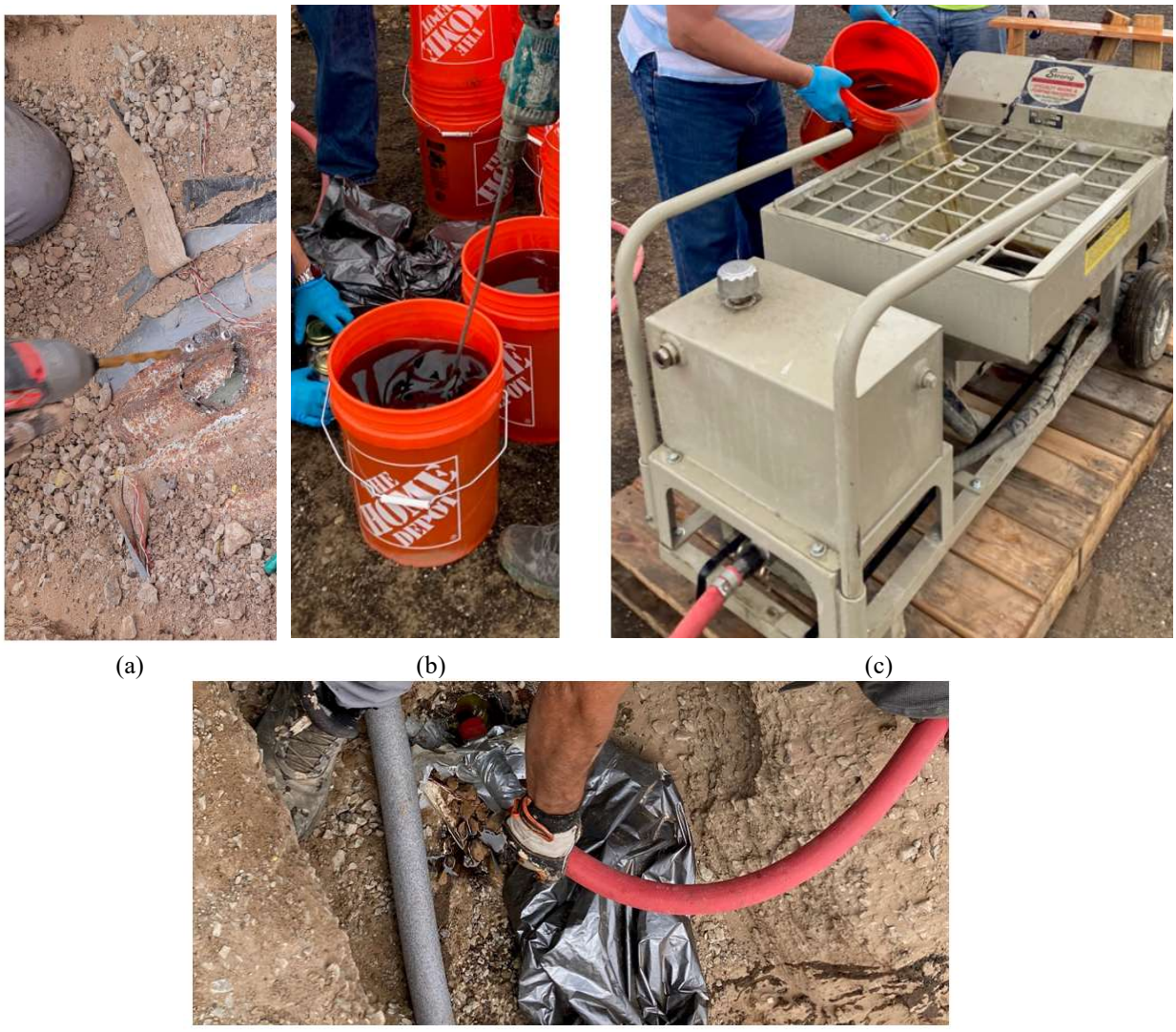

(a) (b) (c)

(d)

FIGURE 23 Mixing and pumping polymer in the annular space using an opening at the middle of the span. (a) perforation to inject polymer. (b) polymer mixing. (c) polymer pumping. (d) polymer injection.

5.2.6 Retrofitted Culvert Load Testing

The retrofitted corroded corrugated metal culvert was left to cure for a week before load testing was performed. Before testing, the truck was weighed on a weighing scale similar to that shown in Figure 13. First, an empty truck with a total weight of 26.1 kips traveled twice over the center of the culvert, with the wheels aligned with the exterior sensor arrays. Then, the truck was filled with sand, to a total weight of 57.05 kips, and traveled on the same path over the culvert. After that, the loaded truck traveled near one of the ends of the culvert, with the interior wheels of the truck aligned with the exterior array of sensors. Finally, the loaded truck traveled near the other end of the culvert, with the interior wheels of the truck aligned with the exterior array of sensors. The breakdown of each wheel load and travel paths are presented in Figure 23.

Figure 24 shows sample of both longitudinal and tangential strains for each load case. The arrival of the first and second axels of the truck could be observed in the spike and dilation of the measured strains. Since the retrofitted culvert has a much higher stiffness than the corrugated metal pipe

alone, the impact of vibration was not observed as significant in the case of the retrofitted pipe compared with the bar corrugated metal pipe. Moreover, the loaded truck case has significantly higher strains than the unloaded case, specifically near the top of the retrofitting GFRP pipe. Finally, the loaded culvert did not observe any significant strains in tangential directions. This might be attributed to the composite action between the GFRP and the corrugated metal pipe. The full data from this testing is presented in Appendix A, Figures A-10 to A-24. The strains measured were consistent with the range of strains predicted by the FE model, which were in the order of 50 microstrains, also lower than the strains of the corroded culvert case.

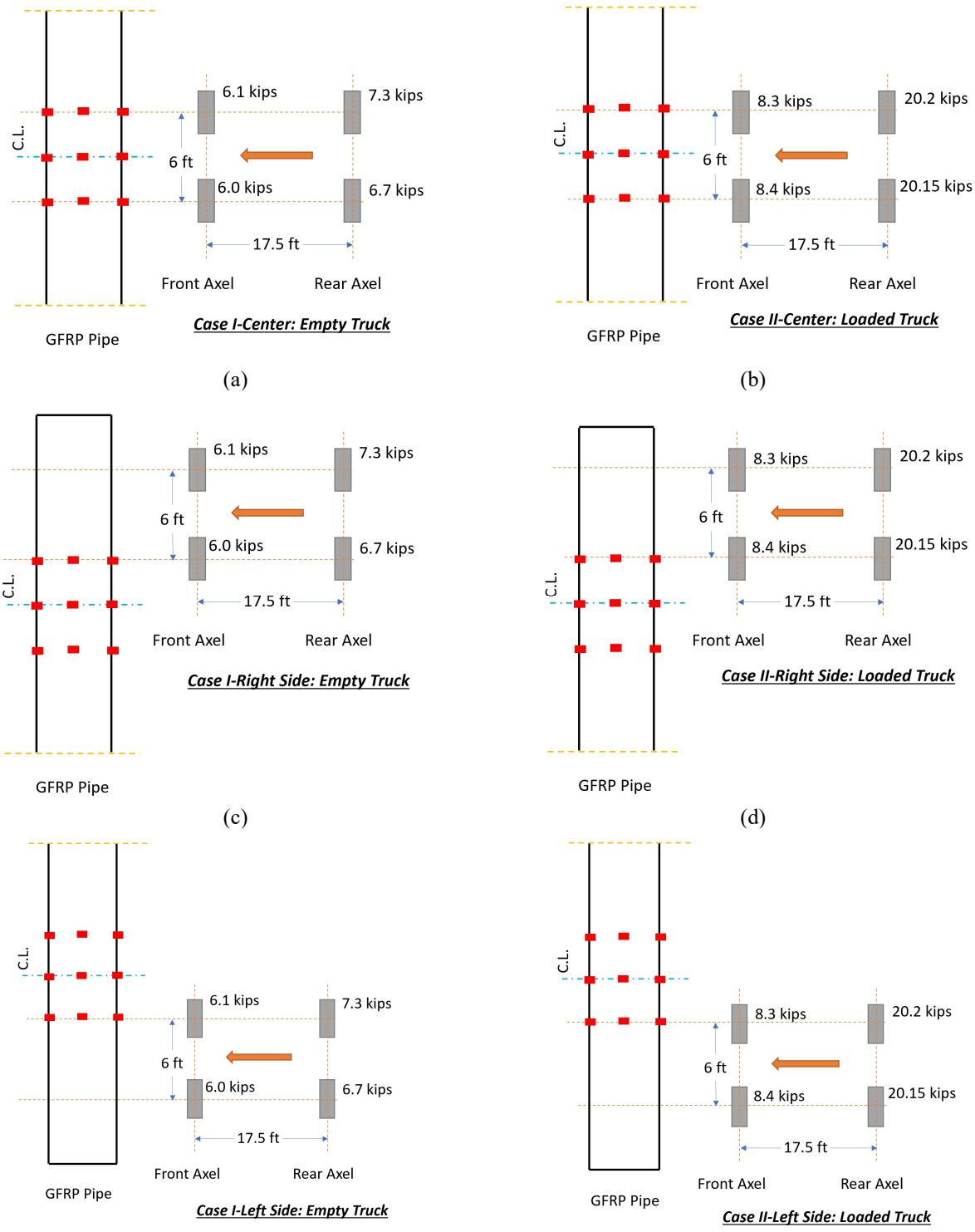

FIGURE 24 Load testing cases for GFRP retrofitting pipe culvert buried at 18 inch depth. (a) Case I-center. Empty truck. (b) Case II-center. Loaded truck. (c) Case I-right side. Empty truck. (d) Case II-right side. Loaded truck. (e) Case I-left side. Empty truck. (f) Case II-left side. Loaded truck.

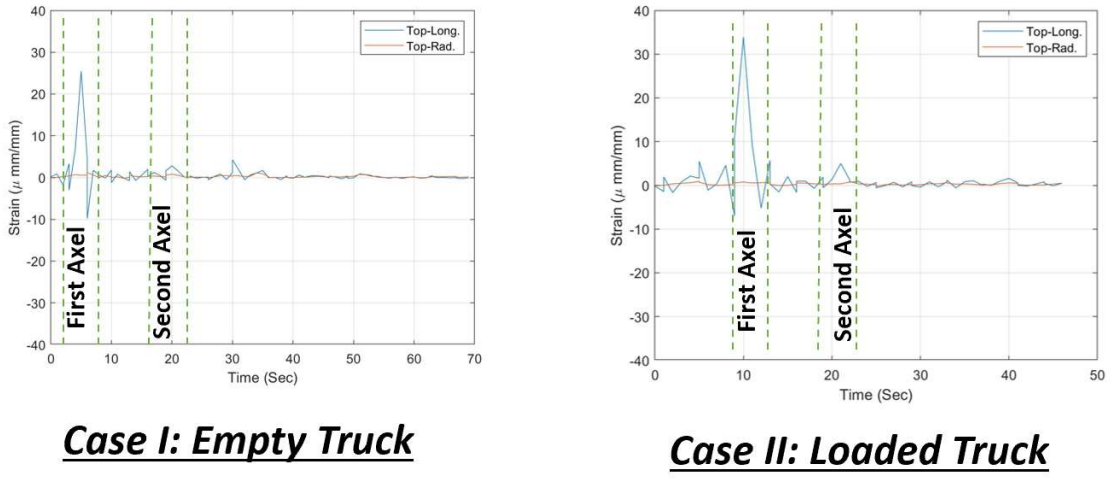

(a) (b)

FIGURE 25 Retrofitted culvert loading test GFRP sample data. (a) Case I. Empty truck. (b) Case II. Loaded truck.

6. CONCLUSIONS

A retrofit design method of corroded corrugated metal pipes using GFRP slip liner was introduced, designed and field implemented. The GFRP slip liner was bonded to CMP using a polymer grout. The design method considered both structural and hydraulic design requirements including wall thrust, buckling, deflection, and bending requirements. The proposed method was used to design a GFRP slip liner to retrofit a 25 ft long and 24 in diameter corroded corrugated metal pipe, with an average thickness of 0.05 in. The corroded corrugated metal pipe was buried under 18 in of soil. With a 1.5 in grout thickness, the design thickness of GFRP thickness was found to be 0.35 in. The manufactured GFRP pipe was instrumented and slip lined. The GFRP pipe was bonded to the corroded corrugated metal pipe using polyester-based polymer. The corroded corrugated metal pipe culvert was tested before and after the retrofitting process via truckload. Testing proved that the GFRP slip liner bonded with the corroded corrugated metal pipe, improving its stiffness, and resisting the loads as a composite section. Testing proved that the proposed method achieves a structural integrity necessary to retrofit the corroded corrugated metal pipe and extend its service life.

REFERENCES

1. Sezen, H.; Yeau, K.Y.; Fox, P.J. In-Situ Load Testing of Corrugated Steel Pipe-Arch Culverts. *Journal of Performance of Constructed Facilities* **2008**, *22*, 245–252, doi:10.1061/(asce)0887-3828(2008)22:4(245).

2. Chennareddy, Rahulreddy. Retrofit of Corroded Metal Culverts Using GFRP Slip-Liner, The University of New Mexico, 2019.

3. FHWA *Status of the Nation's Highways, Bridges, and Transit: Conditions and Performance*; 2006;

4. Maher, M.; Hebeler, G.; Fuggle, A. *Service Life of Culverts*; 2015;

5. Ballinger, C.A.; Drake, P.G. *Culvert Repair Practices Manual. Vol. 2*; 1995;

6. Mitchell, G.F.; Masada, T.; Sargand, S.M.; Tarawneh, B.; Stewart, K.; Mapel, S.; Roberts, J. Risk Assessment and Update of Inspection Procedures for Culverts. *(No. FHWA/OH-2005/002).* **2005**.

7. Sutliff, K. *Caltrans Supplement to FHWA Culvert Repair Practices Manual.*; 2003;

8. Allouche, E.N.; Moore, I.D.; Petersen, L. *Culvert Rehabilitation to Maximize Service Life While Minimizing Direct Costs and Traffic Disruption.*; 2007;

9. Perrin Jr, J.; Jhaveri, C.S. *The Economic Costs of Culvert Failures*; 2004; Vol. 1500;.

10. Wyant, D.C. *Assessment and Rehabilitation of Existing Culverts (Vol. 303).*; Transportation Research Board., 2002;

11. Wagener, B.; E. Leagjeid, E. *Culvert Repair Best Practices , Speci Cations and Special Provisions − Best Practices Guidelines*; 2014;

12. Abolmaali, A.; Mothari, A. *Evaluation of HDPE Pipelines Structural Performance*; 2010;

13. Gassman, S.L.; Schroeder, A.J.; Ray, R.P. Field Performance of High Density Polyethylene Culvert Pipe. *Journal of Transportation Engineering* **2005**, *131*, 160–167, doi:10.1061/(ASCE)0733-947X(2005)131:2(160).

14. Mathews, J.C. *Decision Analysis Guide for Corrugated Metal Culvert Rehabilitation and Replacement Using Trenchless Technology*; 2012;

15. Bakis, C.E.; Bank, L.C.; Brown, V.L.; Cosenza, E.; Davalos, J.F.; Lesko, J.J.; Machida, A.; Rizkalla, S.H.; Triantafillou, T.C. Fiber-Reinforced Polymer Composites for Construction - State-of-the-Art Review. *Perspectives in Civil Engineering: Commemorating the 150th Anniversary of the American Society of Civil Engineers* **2003**, *6*, 369–383, doi:10.1061/(asce)1090-0268(2002)6:2(73).

16. Soudki, K.; Alkhrdaji, T. *Guide for the Design and Construction of Externally Bonded FRP Systems for Strengthening Concrete Structures (ACI 440.2R-02)*; 2005;

17. Park, J.S.; Hong, W.H.; Lee, W.; Park, J.H.; Yoon, S.J. Pipe Stiffness Prediction of Buried GFRP Flexible Pipe. *Polymers and Polymer Composites* **2014**, *22*, 17–24, doi:10.1177/096739111402200103.

18. Vaslestad, J.; Korusiewicz, L.; Wysokowski, A. General Description of Static and Dynamic Testing of Instrumented Steel Culvert. In Proceedings of the proceedings of the durable and safe road pavements, v international conference; 1999.

19. AASHTO, L. *Bridge Design Specifications 8th Edition.*; Washington, DC, USA., 2017;

20. Das, D.; Dubey, O.P.; Sharma, M.; Nayak, R.K.; Samal, C. Mechanical Properties and Abrasion Behaviour of Glass Fiber Reinforced Polymer Composites – A Case Study. *Materials Today: Proceedings* **2019**, *19*, 506–511, doi:10.1016/j.matpr.2019.07.644.

APPENDIX A: CORRODED CULVERT LOADING DATA

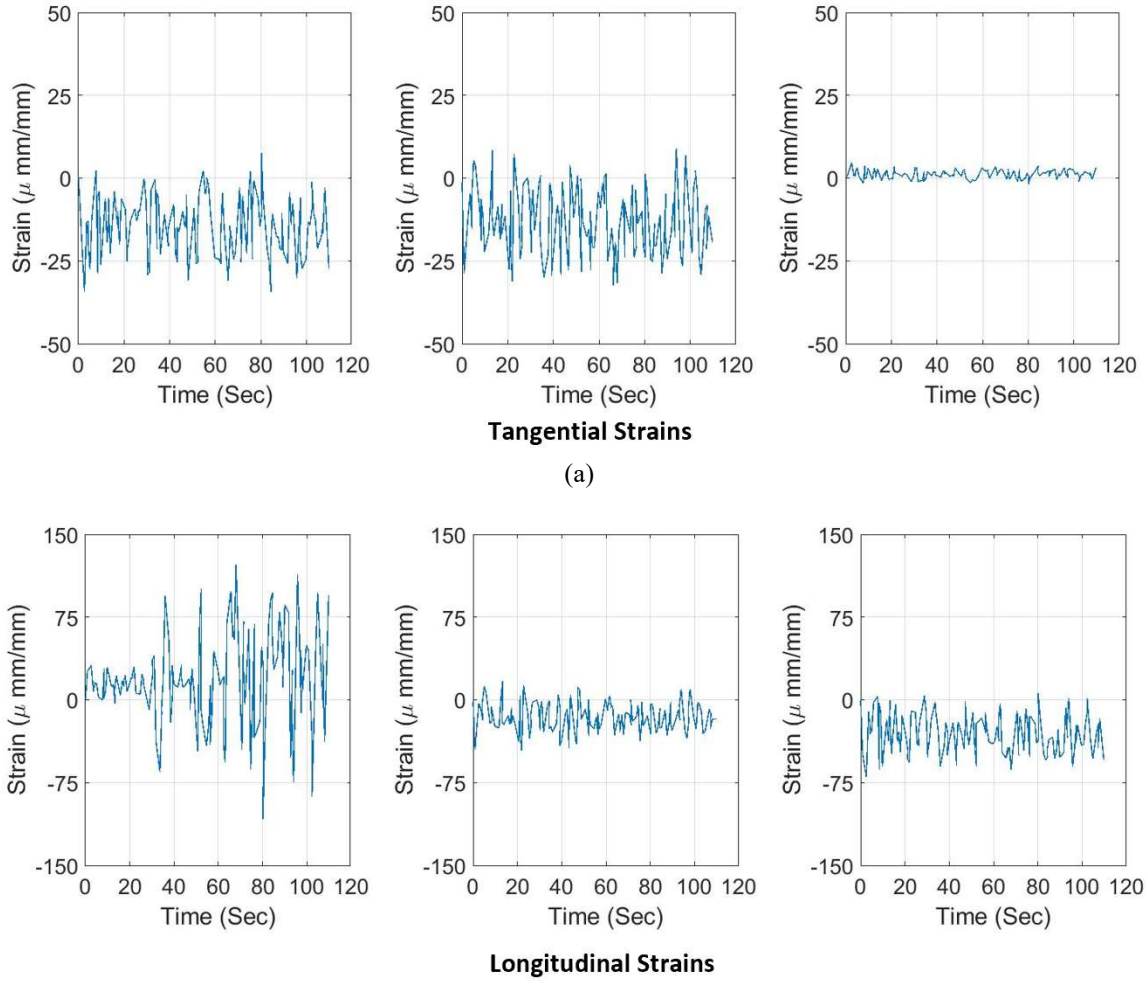

FIGURE 26 Corroded culvert top strains of the empty truck running at center. Strains represented in microstrains (1 me = 10-6 e). (a) tangential strains. (b) longitudinal strains.

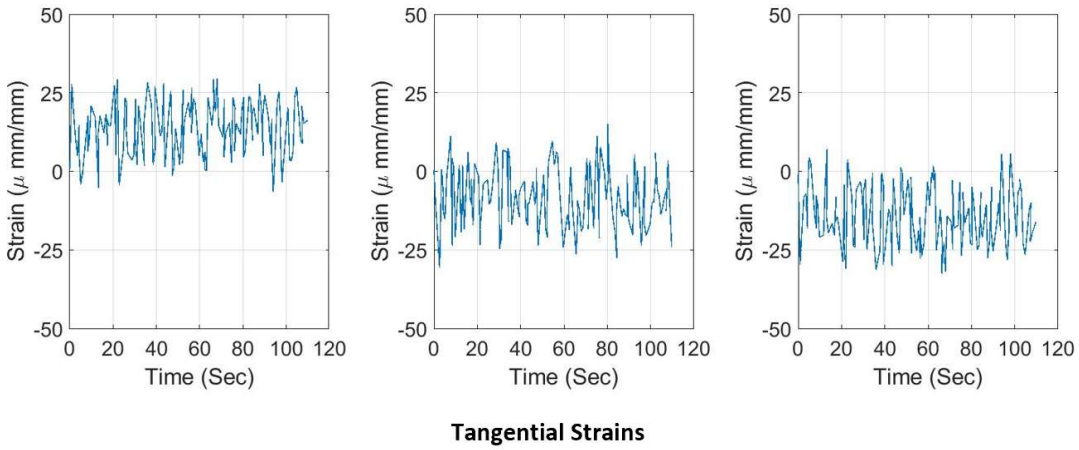

(a)

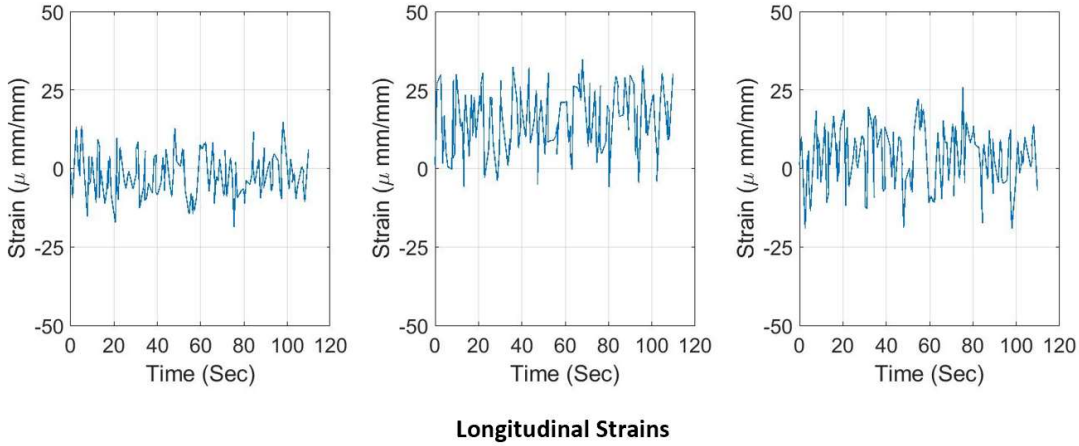

(b)

FIGURE 27 Corroded culvert side strains of the empty truck running at center. Strains represented in microstrains (1 me = 10-6 e). (a) tangential strains. (b) longitudinal strains.

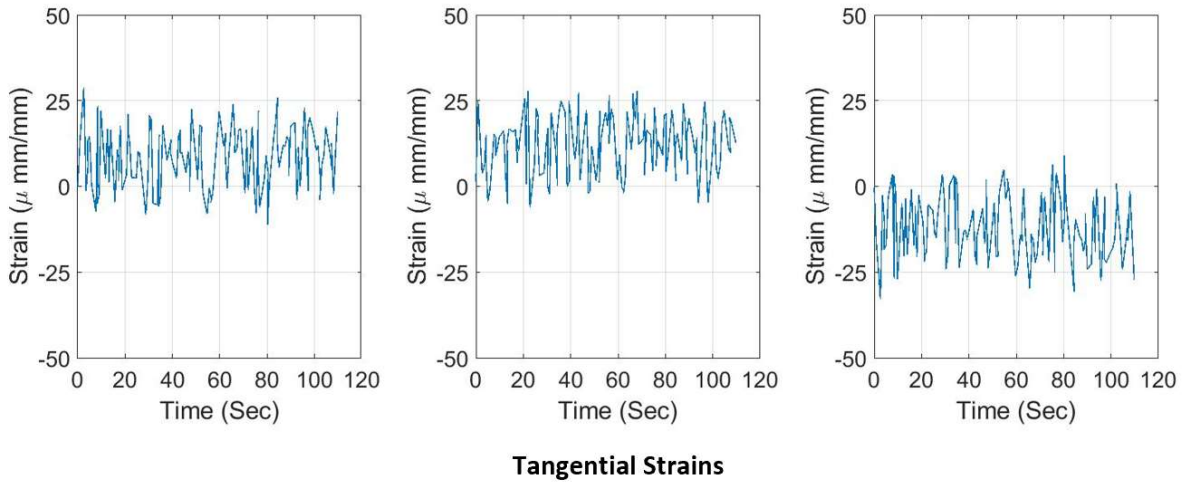

(a)

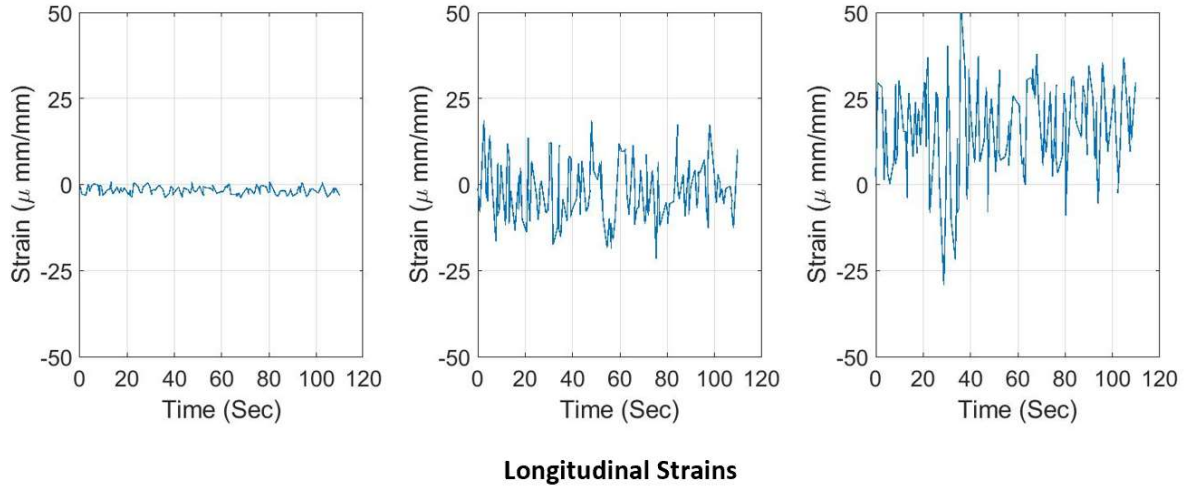

(b)

FIGURE 28 Corroded culvert bottom strains of the empty truck running at center. Strains represented in microstrains (1 me = 10-6 e). (a) tangential strains. (b) longitudinal strains.

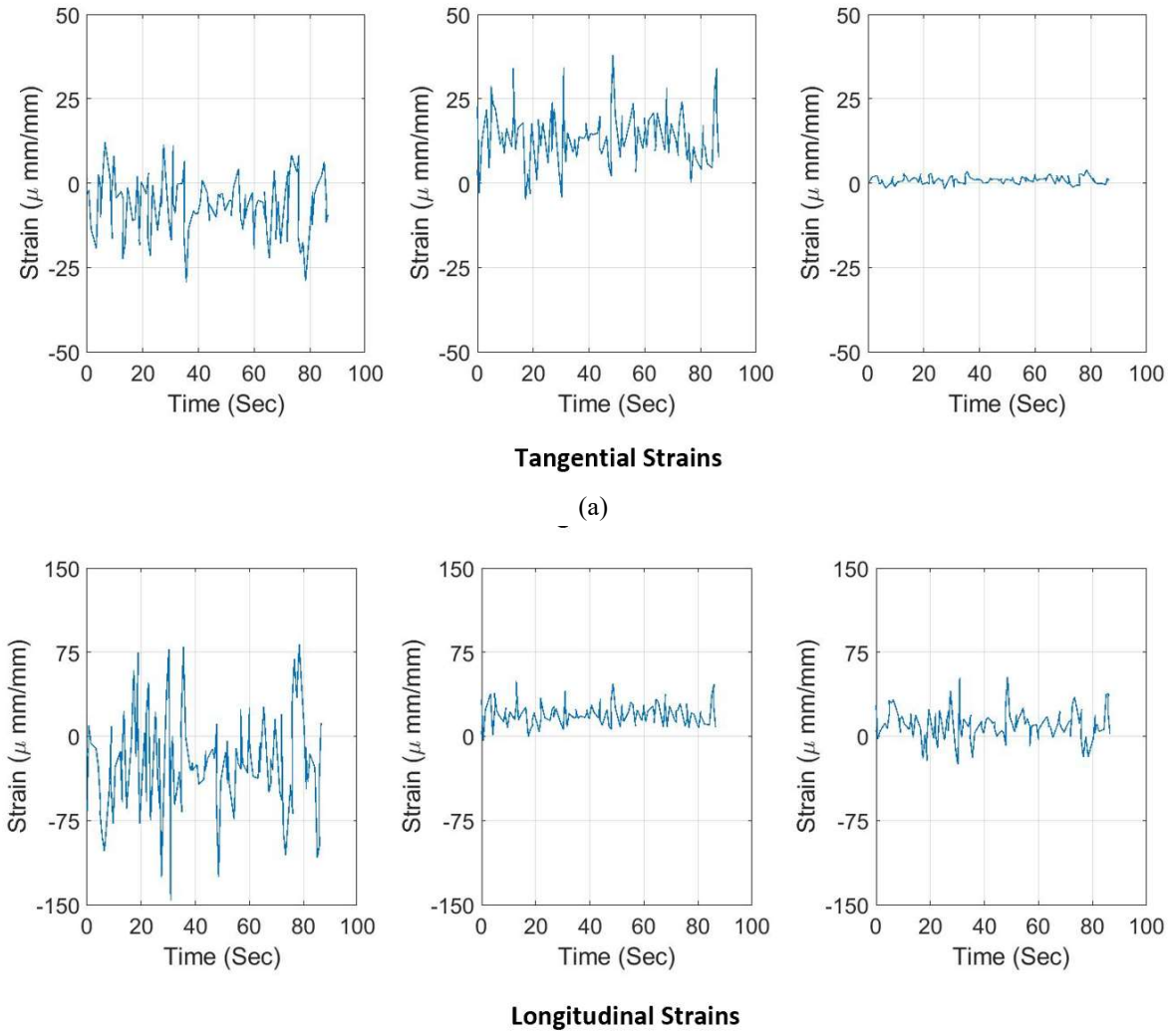

FIGURE 29 Corroded culvert top strains of the loaded truck running at center. Strains represented in microstrains (1 me = 10-6 e). (a) tangential strains. (b) longitudinal strains.

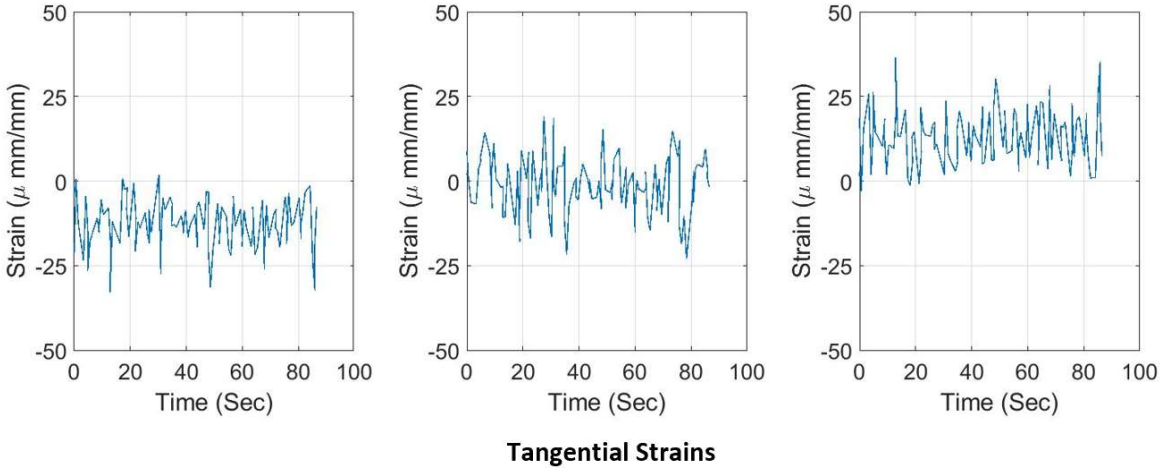

(a)

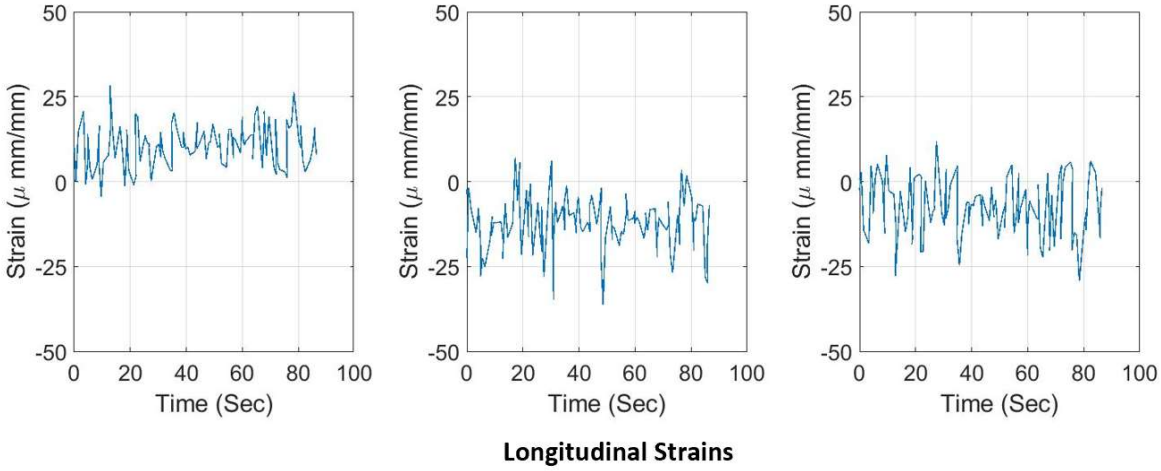

(b)

FIGURE 30 Corroded culvert side strains of the loaded truck running at center. Strains represented in microstrains (1 me = 10-6 e). (a) tangential strains. (b) longitudinal strains.

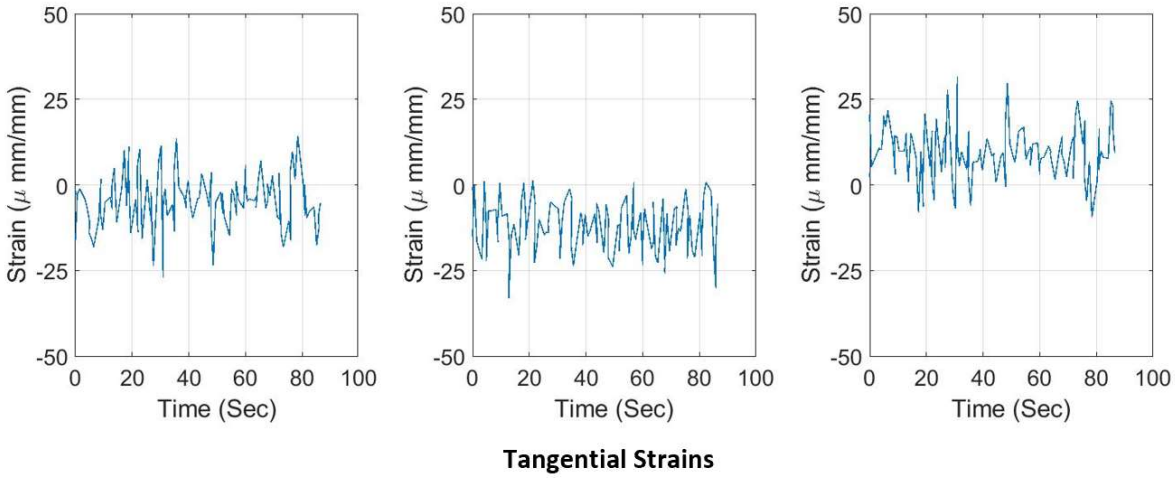

(a)

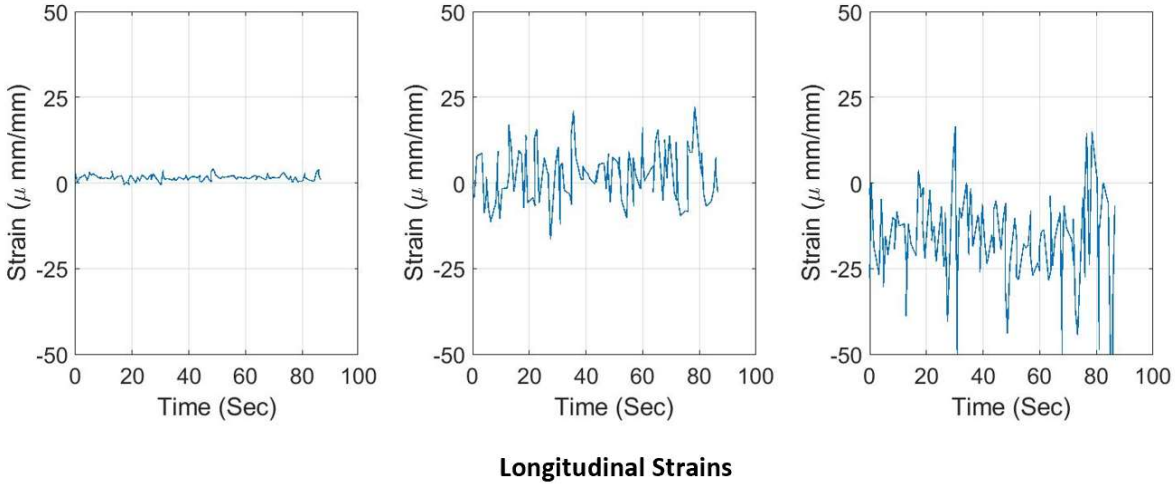

(b)

FIGURE 31 Corroded culvert bottom strains of the loaded truck running at center. Strains represented in microstrains (1 me = 10-6 e). (a) tangential strains. (b) longitudinal strains.

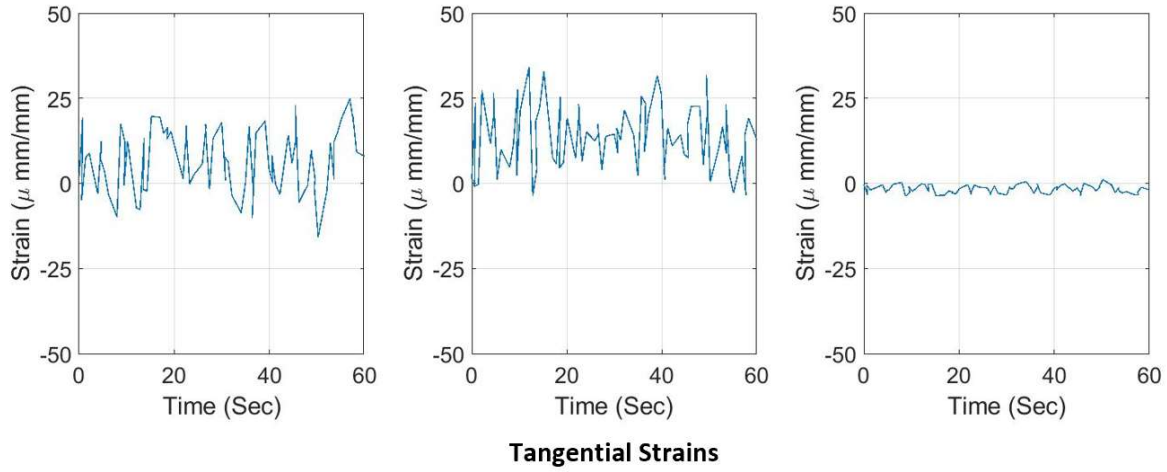

(a)

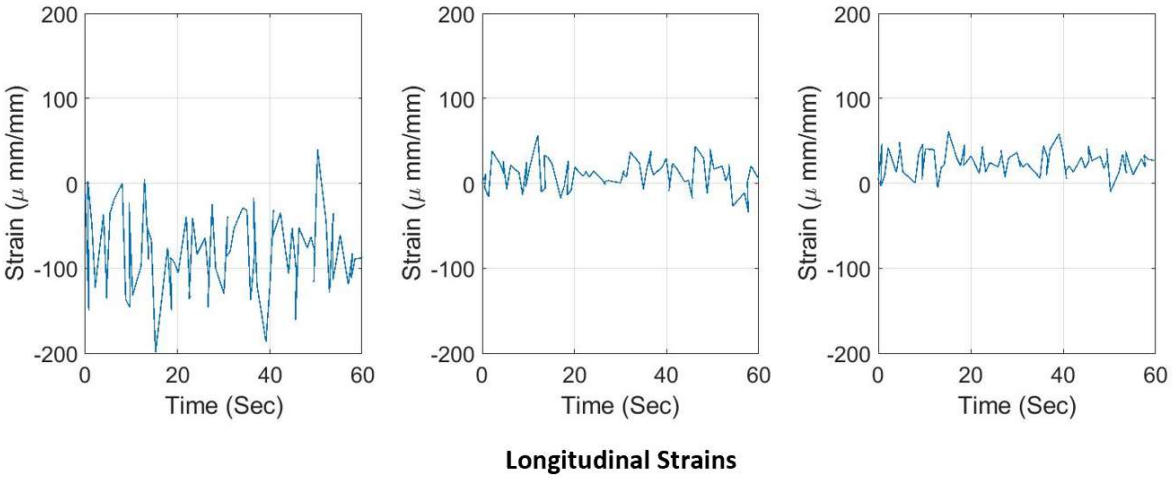

(b)

FIGURE 32 Corroded culvert top strains of the loaded truck running at right. Strains represented in microstrains (1 me = 10-6 e). (a) tangential strains. (b) longitudinal strains.

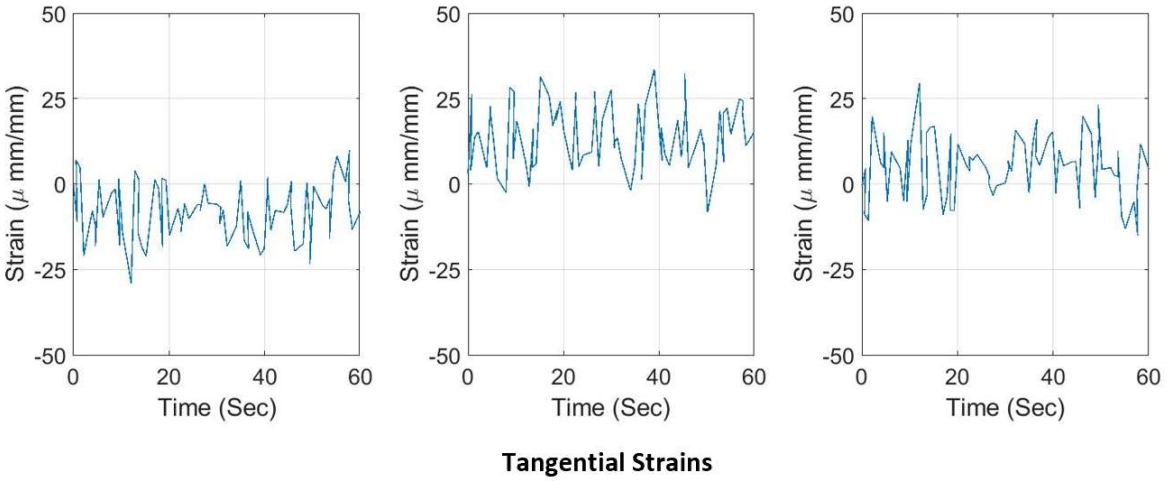

(a)

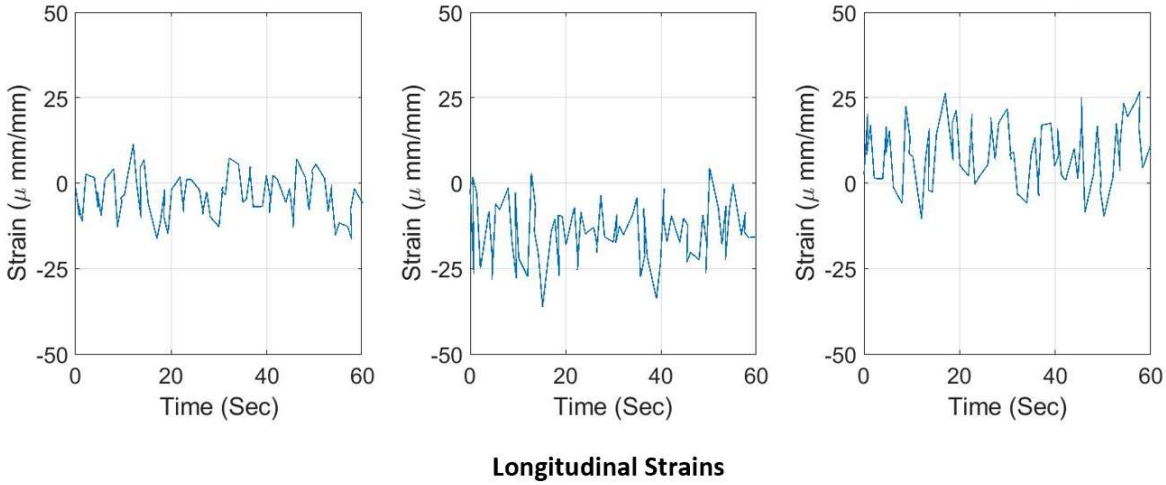

(b)

FIGURE 33 Corroded culvert side strains of the loaded truck running at right. Strains represented in microstrains (1 me = 10-6 e). (a) tangential strains. (b) longitudinal strains.

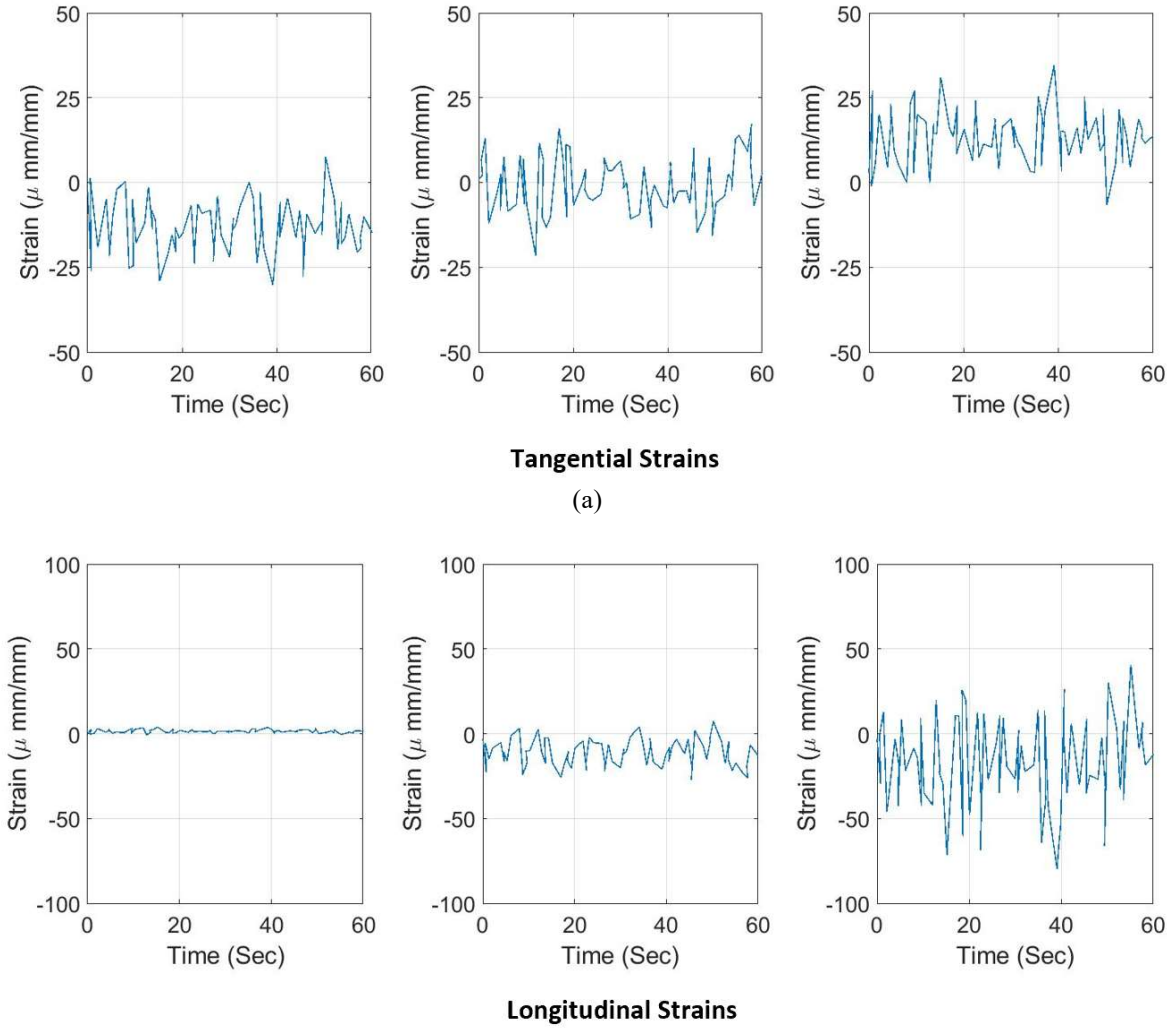

FIGURE 34 Corroded culvert bottom strains of the loaded truck running at right. Strains represented in microstrains (1 me = 10-6 e). (a) tangential strains. (b) longitudinal strains.

APPENDIX B: RETROFITTED CULVERT LOADING DATA

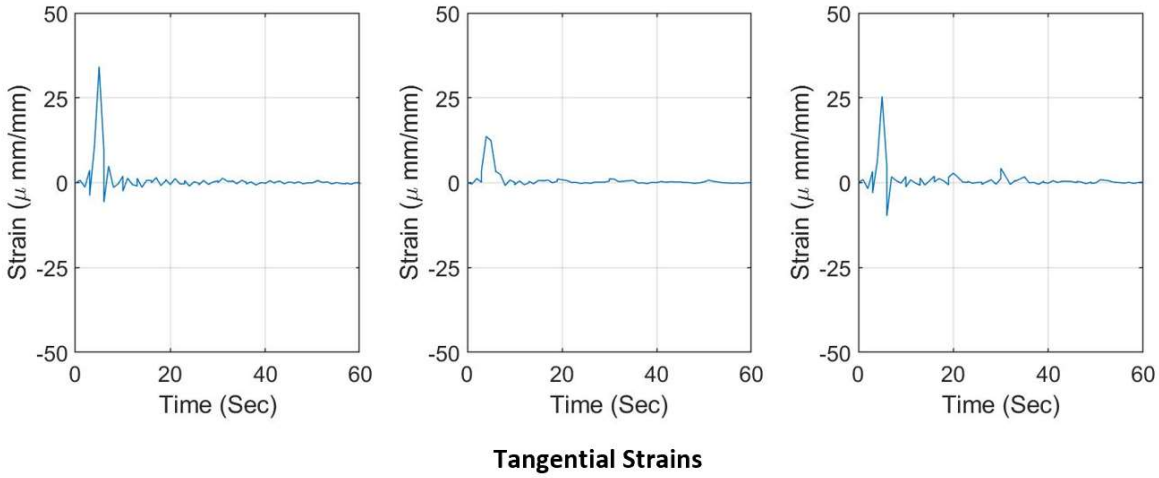

(a)

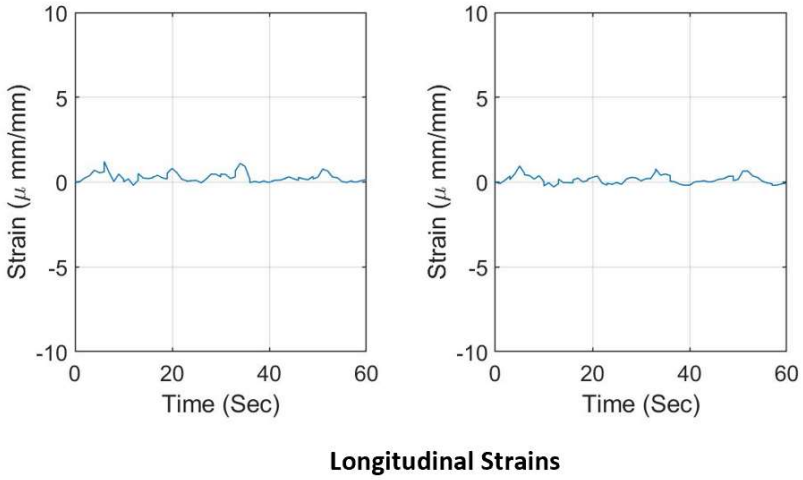

(b)

FIGURE 35 GFRP top strains of the empty truck running at center (Travel 1). Strains represented in microstrains (1 me = 10-6 e). (a) tangential strains. (b) longitudinal strains.

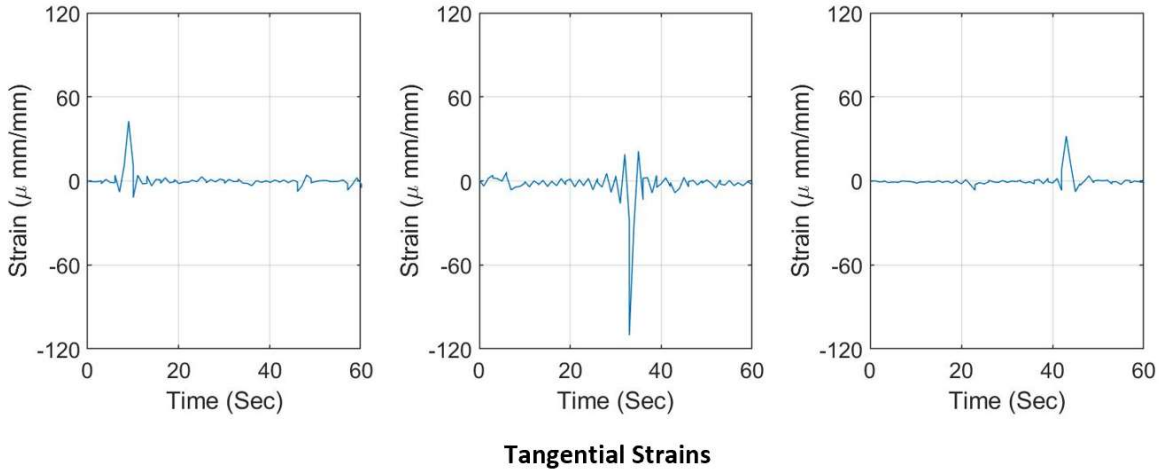

(a)

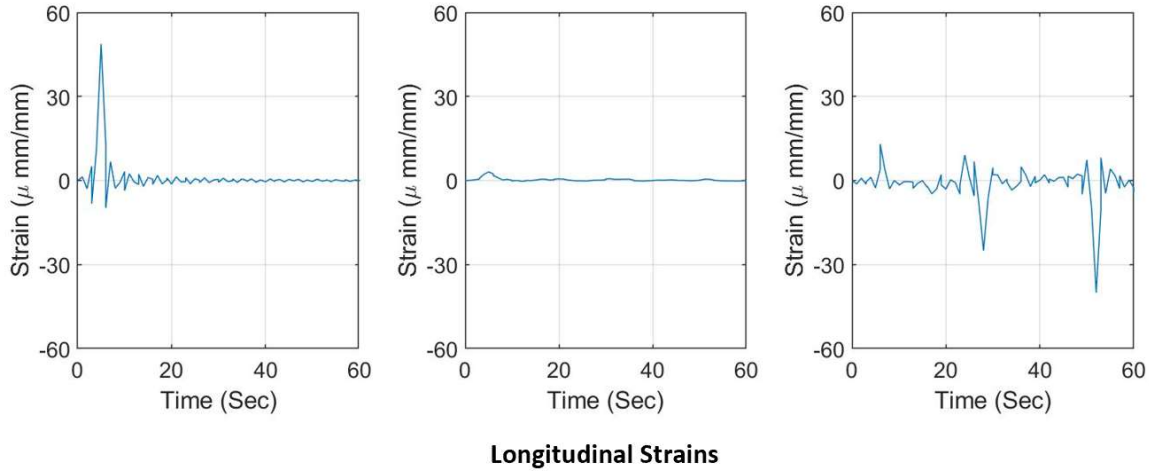

(b)

FIGURE 36 GFRP left side strains of the empty truck running at center (Travel 1). Strains represented in microstrains (1 me = 10-6 e). (a) tangential strains. (b) longitudinal strains.

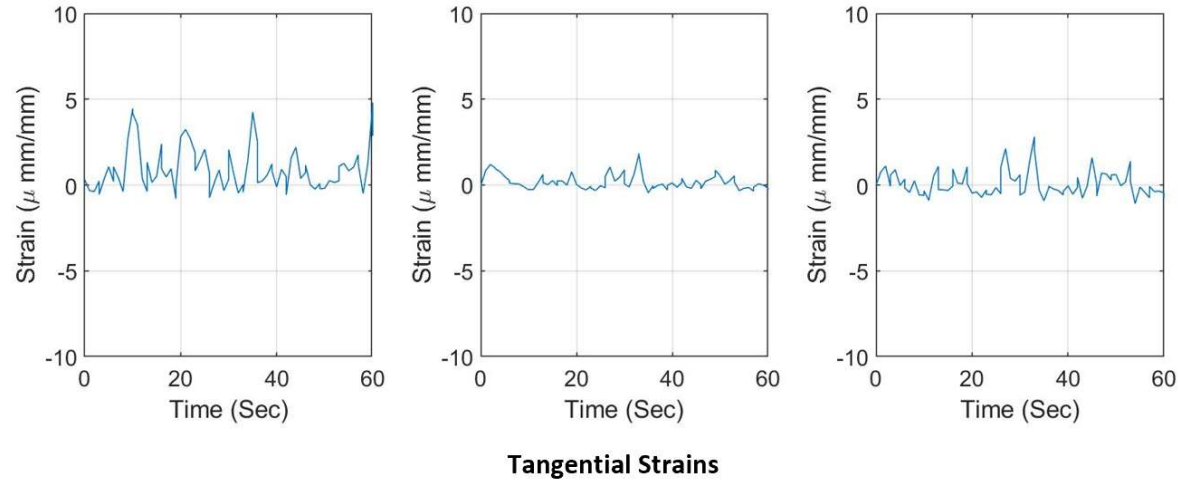

(a)

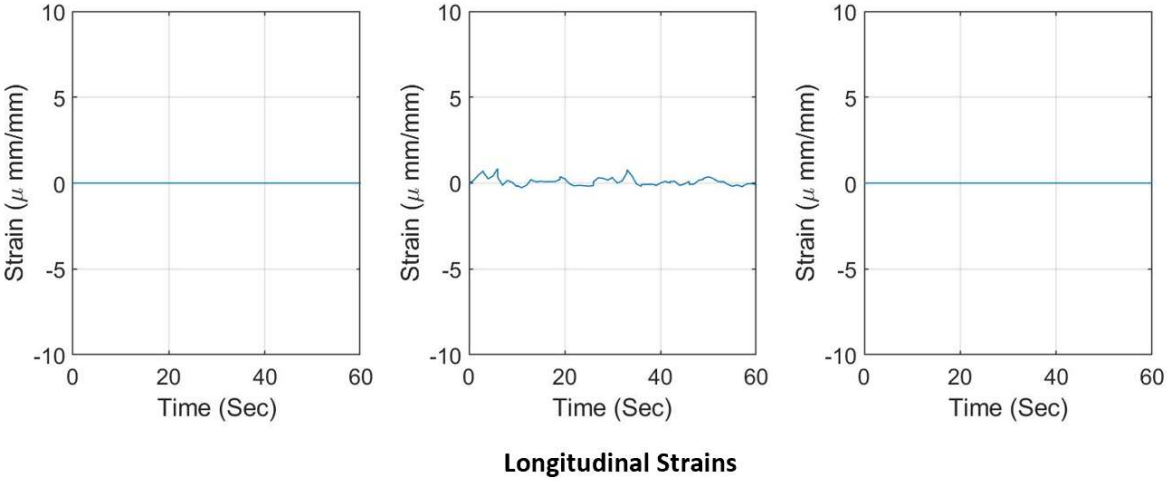

(b)

FIGURE 37 GFRP right side strains of the empty truck running at center (Travel 1). Strains represented in microstrains (1 me = 10-6 e). (a) tangential strains. (b) longitudinal strains.

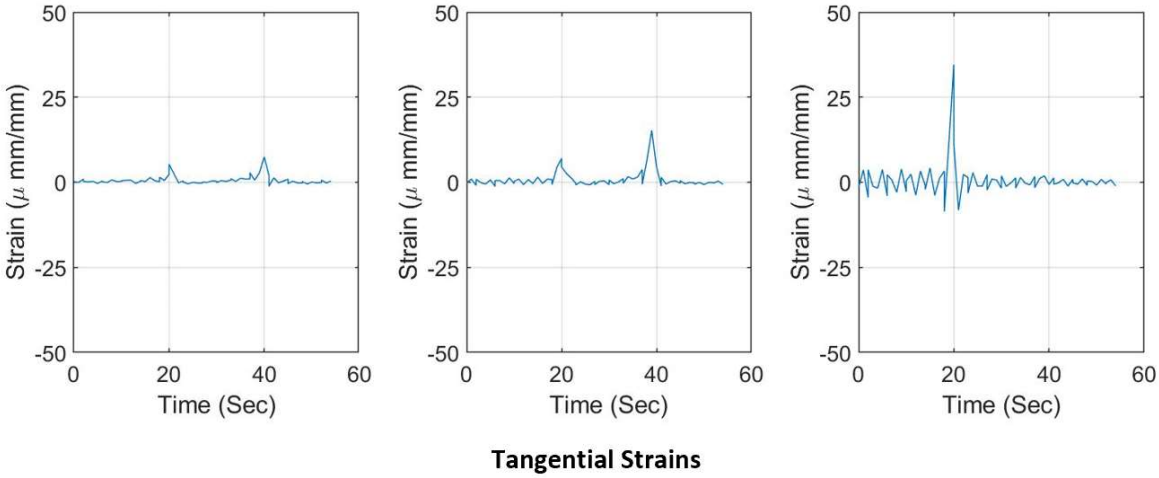

(a)

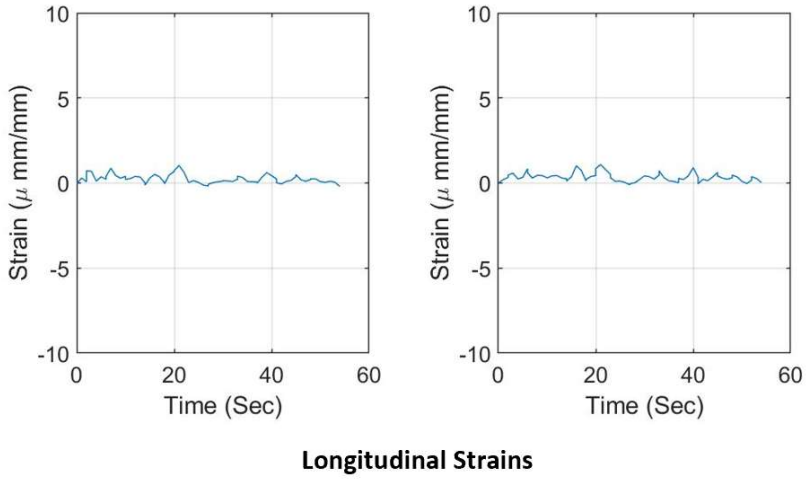

(b)

FIGURE 38 GFRP top strains of the empty truck running at center (Travel 2). Strains represented in microstrains (1 me = 10-6 e). (a) tangential strains. (b) longitudinal strains.

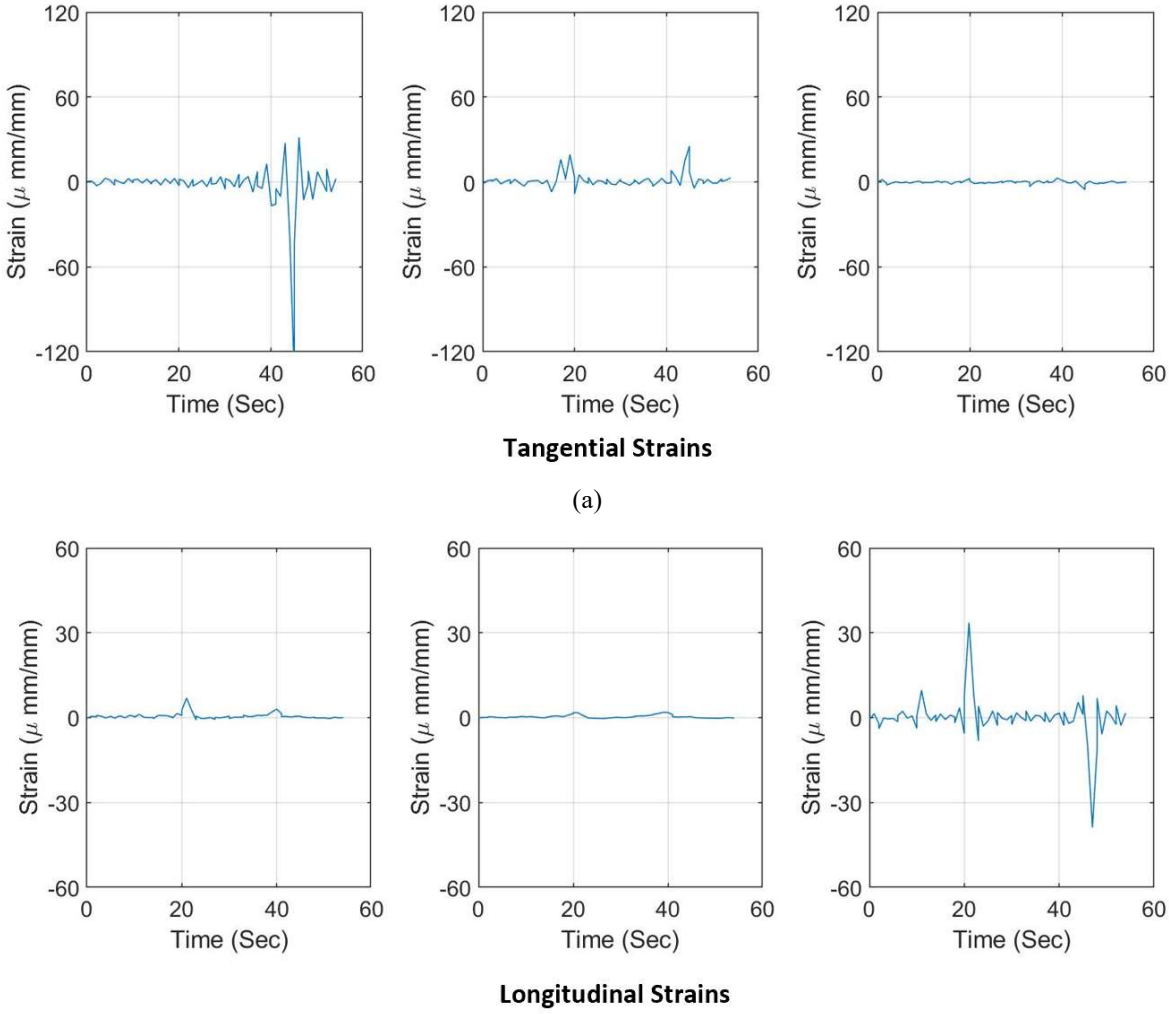

FIGURE 39 GFRP left side strains of the empty truck running at center (Travel 2). Strains represented in microstrains (1 me = 10-6 e). (a) tangential strains. (b) longitudinal strains.

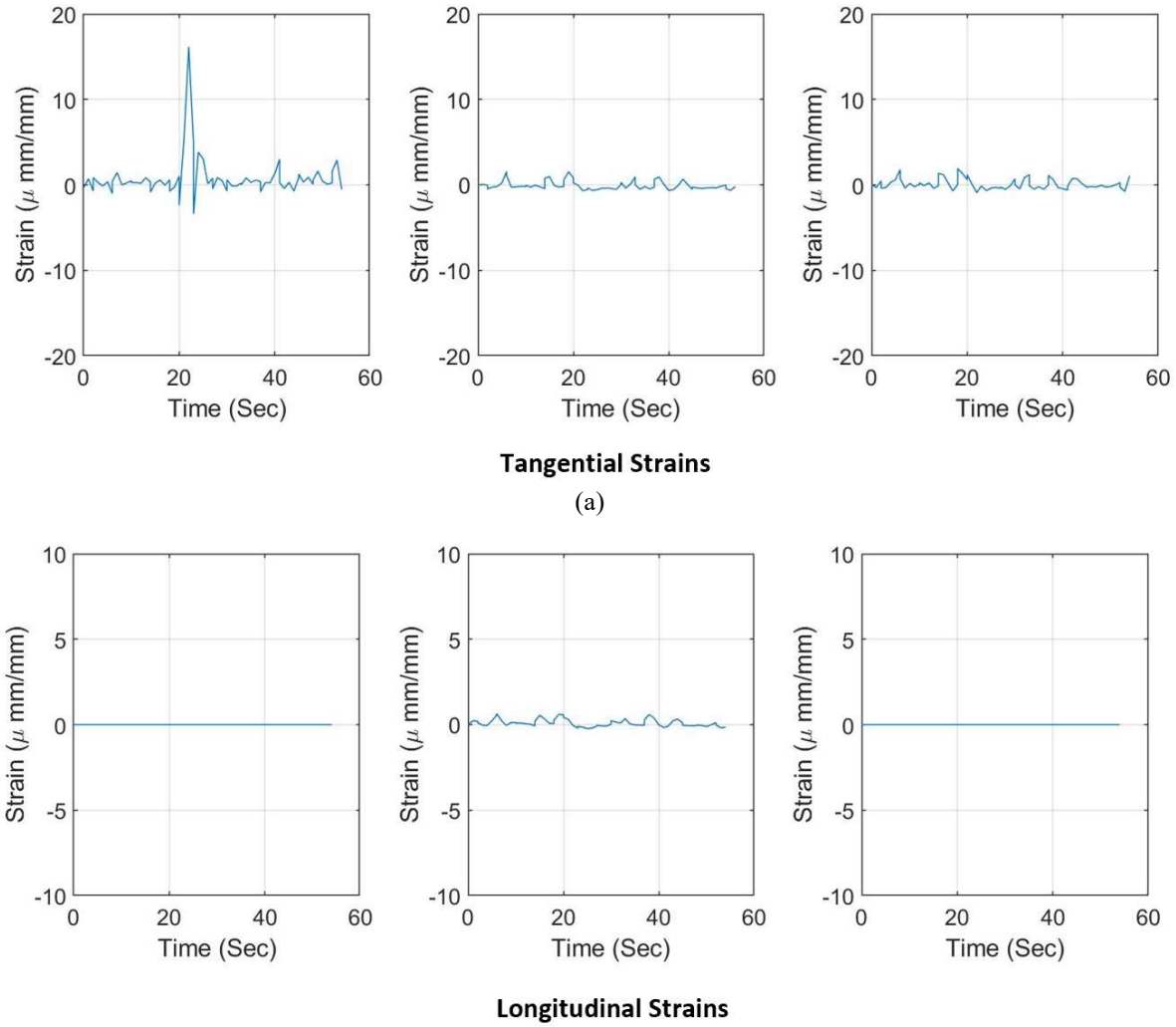

(a)

(b)

FIGURE 40 GFRP right side strains of the empty truck running at center (Travel 2). Strains represented in microstrains (1 me = 10-6 e). (a) tangential strains. (b) longitudinal strains.

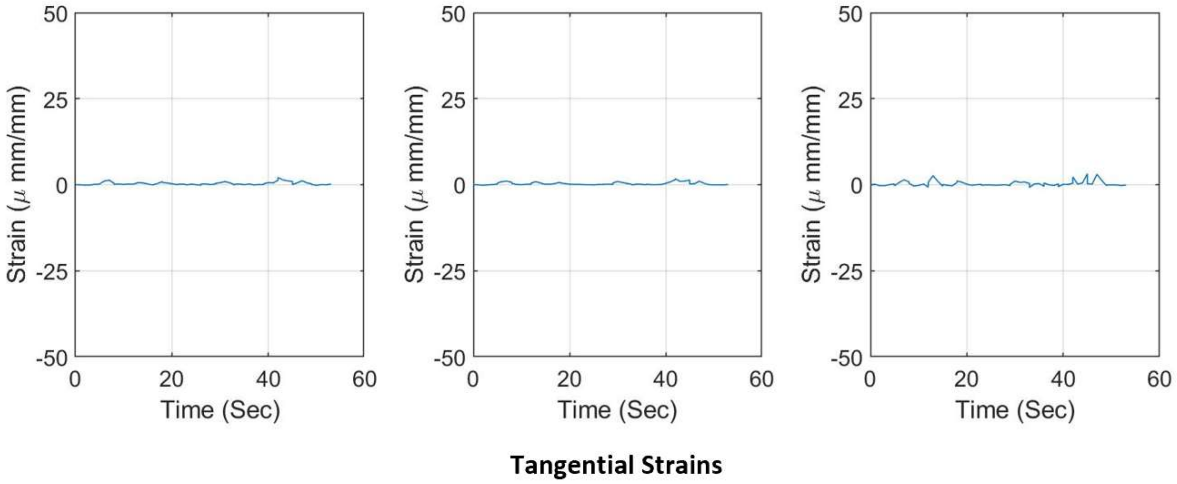

(a)

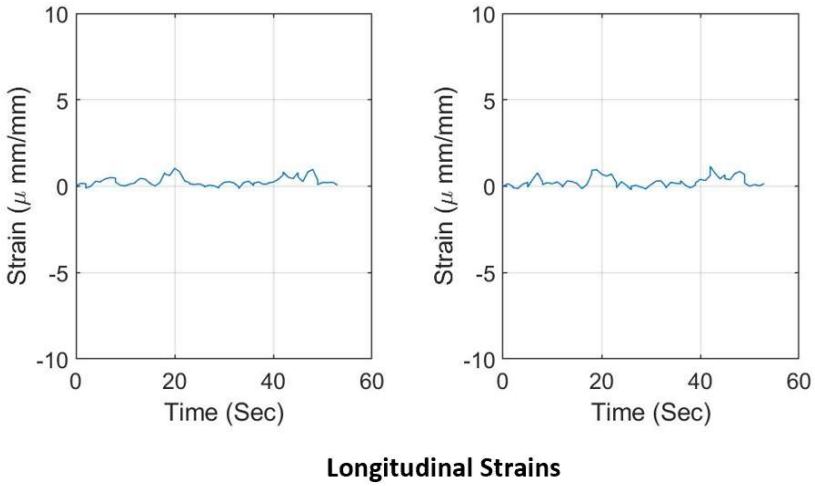

(b)

FIGURE 41 GFRP top strains of the loaded truck running at center. Strains represented in microstrains (1 me = 10-6 e). (a) tangential strains. (b) longitudinal strains.

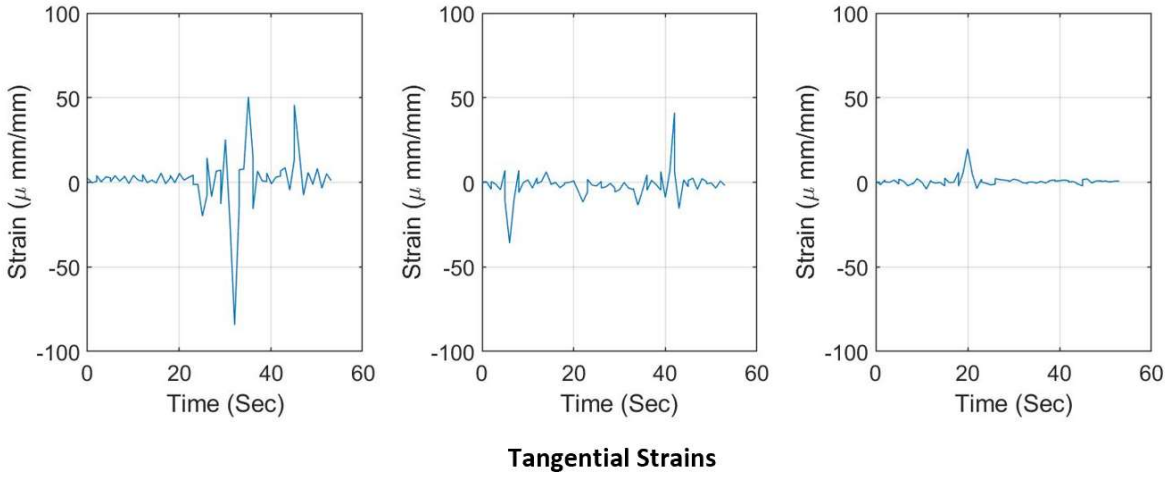

(a)

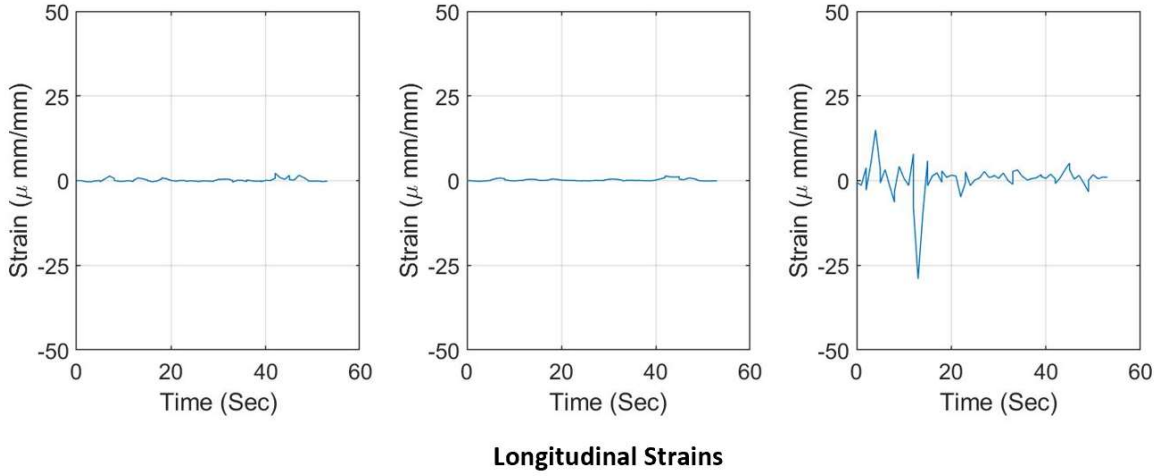

(b)

FIGURE 42 GFRP left side strains of the loaded truck running at center. Strains represented in microstrains (1 me = 10-6 e). (a) tangential strains. (b) longitudinal strains.

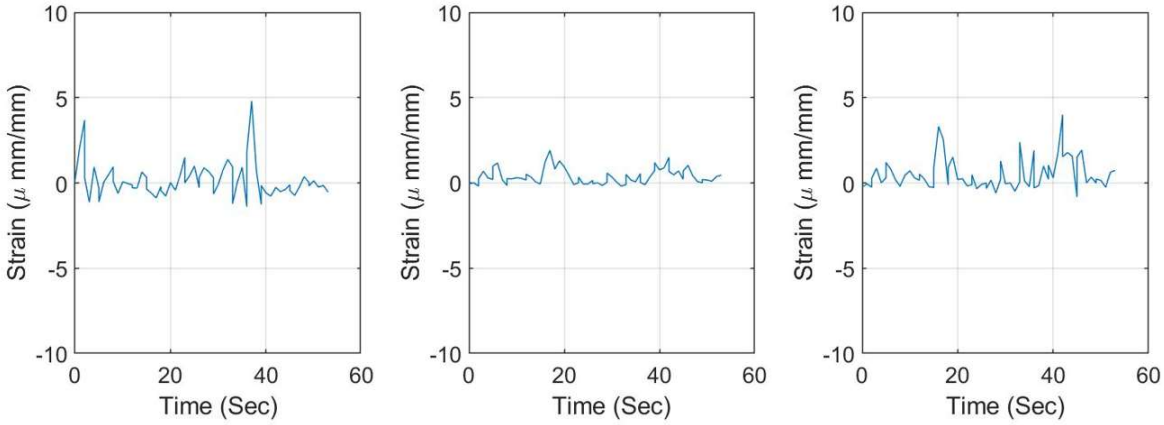

(a)

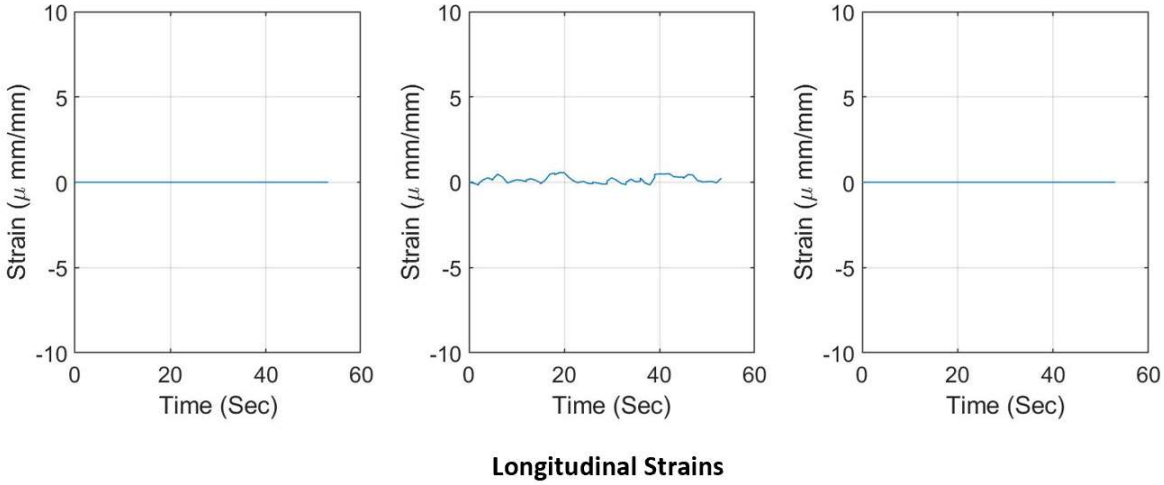

(b)

FIGURE 43 GFRP right side strains of the loaded truck running at center. Strains represented in microstrains (1 me = 10-6 e). (a) tangential strains. (b) longitudinal strains.

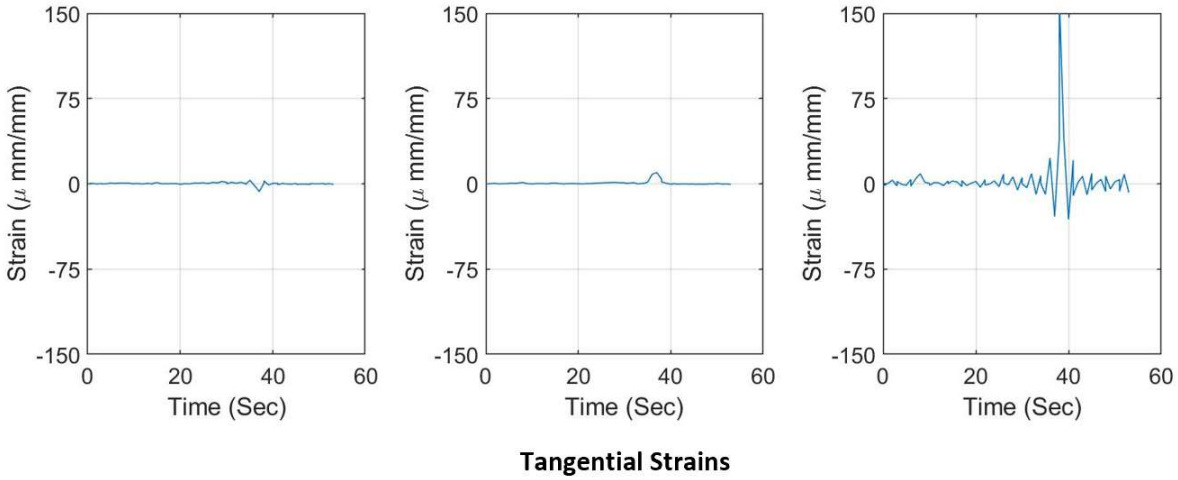

(a)

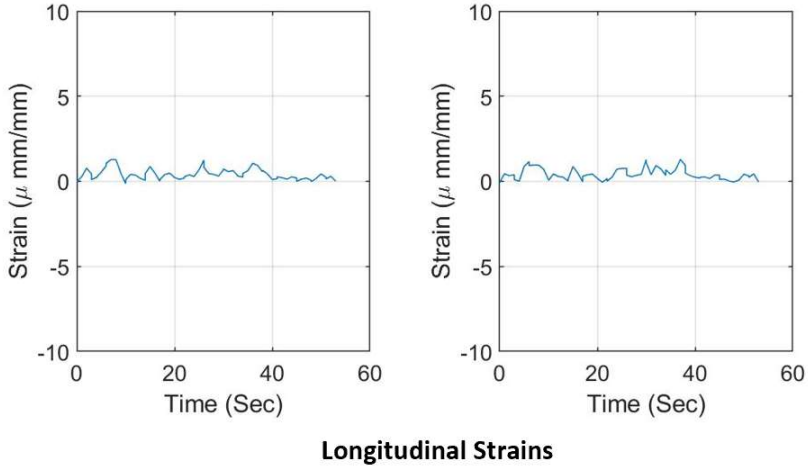

(b)

FIGURE 44 GFRP top strains of the loaded truck running at right. Strains represented in microstrains (1 me = 10-6 e). (a) tangential strains. (b) longitudinal strains.

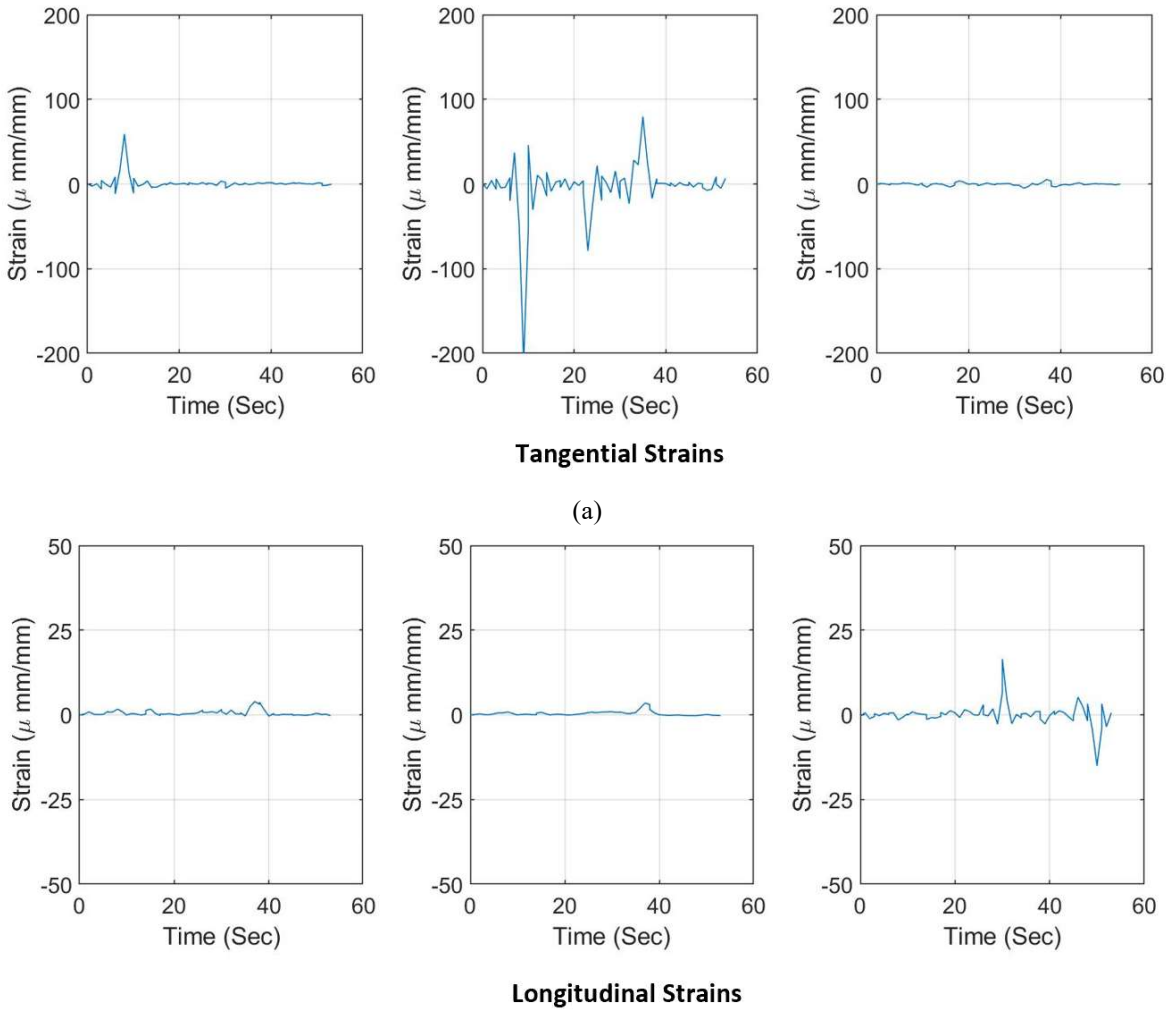

(a)

(b)

FIGURE 45 GFRP left side strains of the loaded truck running at right. Strains represented in microstrains (1 me = 10-6 e). (a) tangential strains. (b) longitudinal strains.

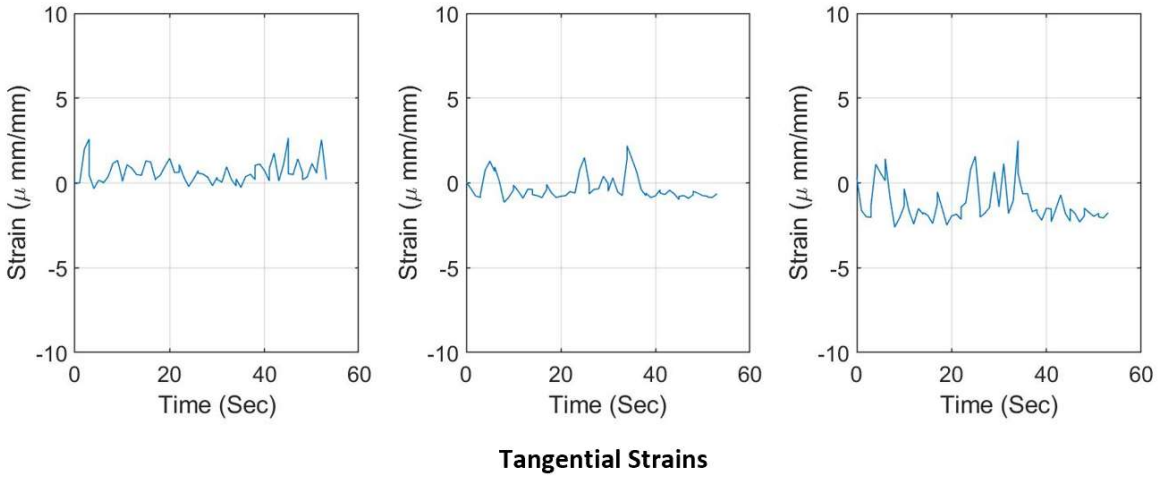

(a)

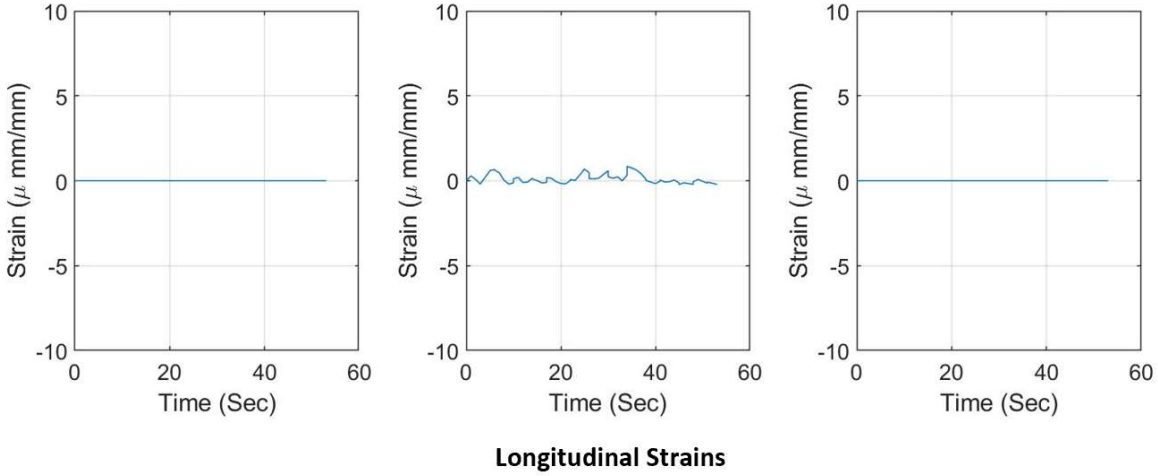

(b)

FIGURE 46 GFRP right side strains of the loaded truck running at right. Strains represented in microstrains (1 me = 10-6 e). (a) tangential strains. (b) longitudinal strains.

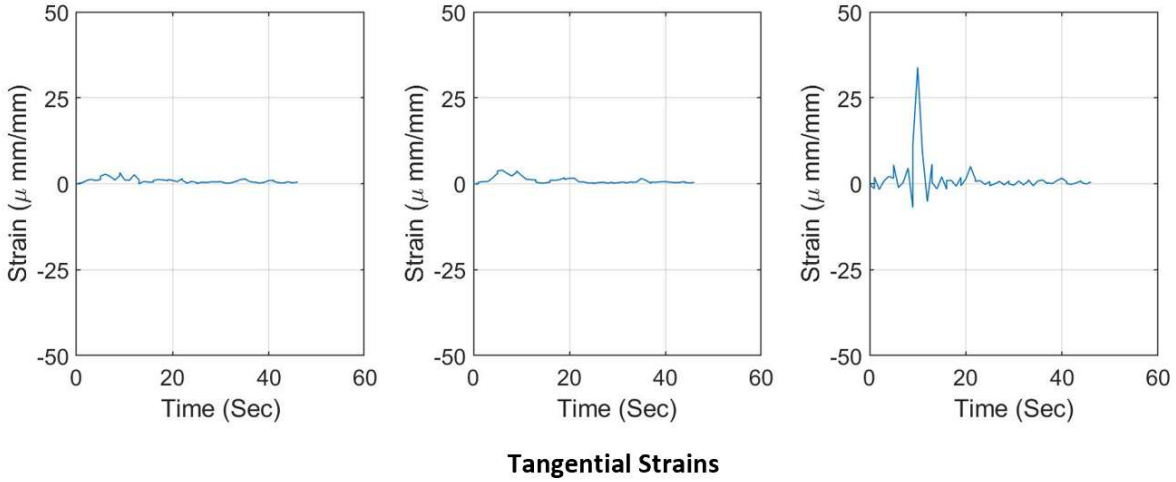

(a)

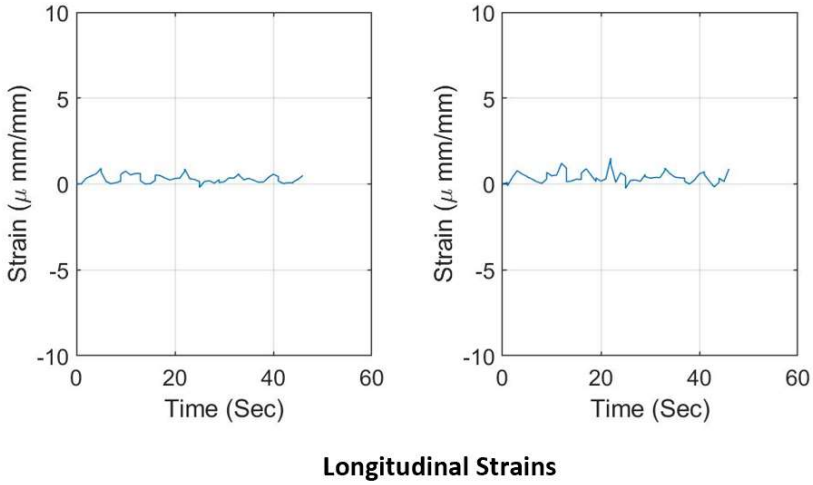

(b)

FIGURE 47 GFRP top strains of the loaded truck running at left. Strains represented in microstrains (1 me = 10-6 e). (a) tangential strains. (b) longitudinal strains.

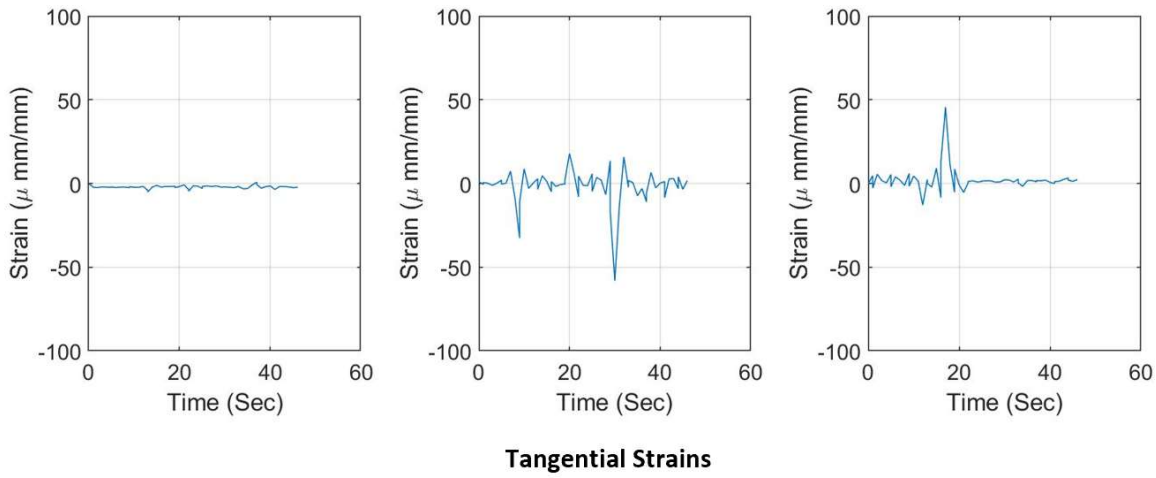

(a)

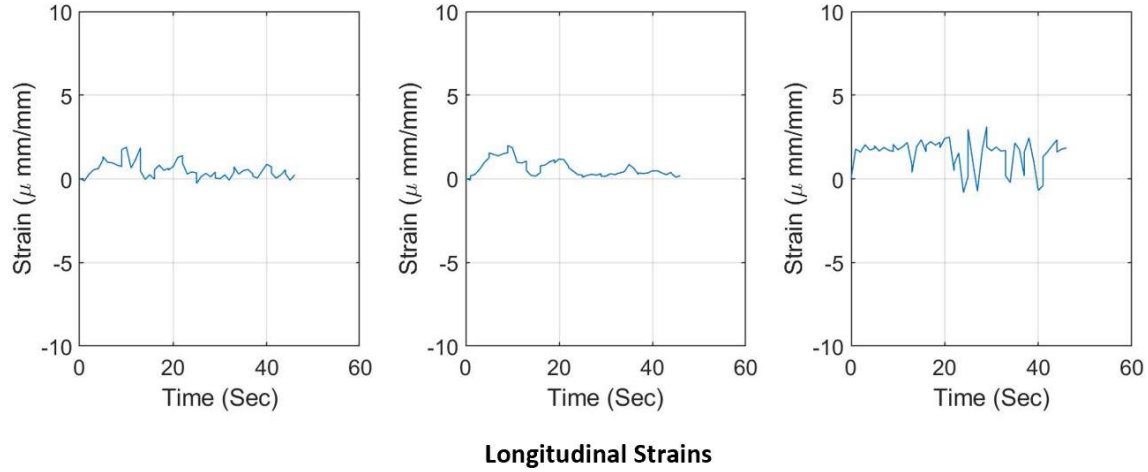

(b)

FIGURE 48 GFRP left side strains of the loaded truck running at left. Strains represented in microstrains (1 me = 10-6 e). (a) tangential strains. (b) longitudinal strains.

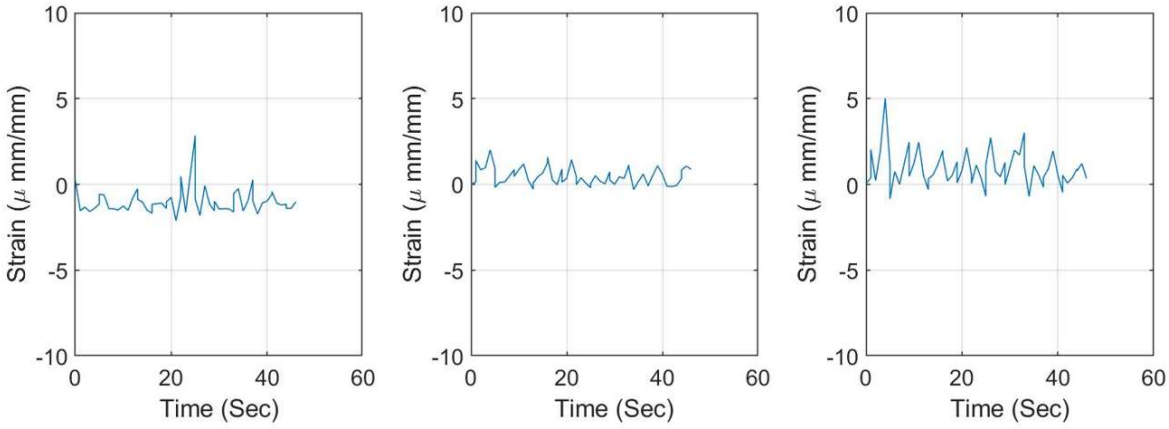

(a)

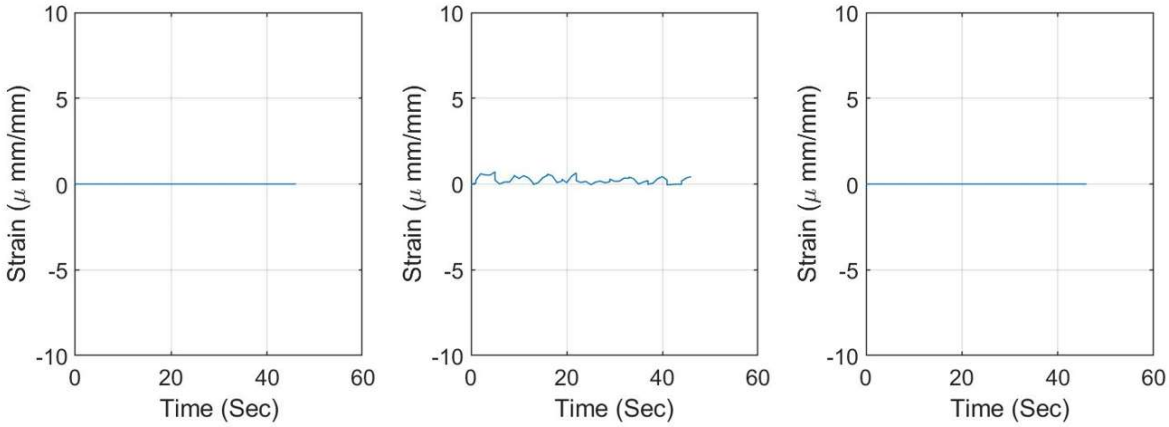

(b)

FIGURE 49 GFRP right side strains of the loaded truck running at left. Strains represented in microstrains (1 me = 10-6 e). (a) tangential strains. (b) longitudinal strains.